3

Radiative Transfer

ALL OF THE information received by a satellite about the Earth and its atmosphere comes in the form of electromagnetic radiation. It is necessary, therefore, to understand the mechanisms by which this radiation is generated and how it interacts with the atmosphere. Several texts listed in the Bibliography explore atmospheric radiation in detail. Here we concentrate on those aspects that are essential for satellite meteorology.

3.1 BASIC QUANTITIES

Electromagnetic radiation consists of alternating electric and magnetic fields (Fig. 3.1). The electric field vector is perpendicular to the magnetic field vector, and the direction of propagation is perpendicular to both. Radiation is often specified by its *wavelength,* which is the distance between crests of the electric or magnetic field. Figure 3.2 shows the electromagnetic spectrum. A broad range of wavelengths from the ultraviolet to the microwave region is useful in satellite meteorology.

An alternate way to describe radiation is to give its *frequency,* which is the rate at which the electric or magnetic field oscillates when observed at a point.

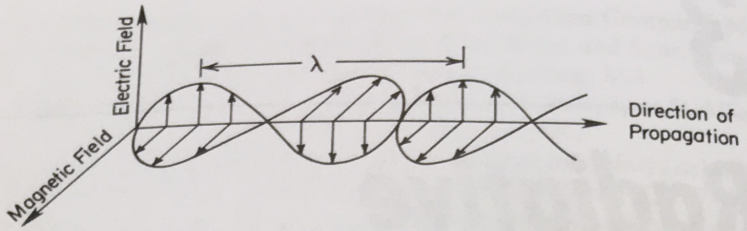

FIGURE 3.1. Schematic representation of electromagnetic waves.

The fundamental unit of frequency is the hertz (Hz), or one cycle per second. The frequency ν is related to the wavelength λ by

$$\nu = \frac{c}{\lambda}, \tag{3.1}$$

where c is the speed with which electromagnetic radiation travels and is known as the *speed of light*. In a vacuum the speed of light is 2.99792458×10^8 m s^{-1}. In the atmosphere, it travels slightly more slowly, due to interaction with air molecules.

The *index of refraction*, n, of a substance is the ratio of the speed of light in vacuum to the speed with which electromagnetic radiation travels in that substance. At sea level, the index of refraction of air is approximately 1.0003. For

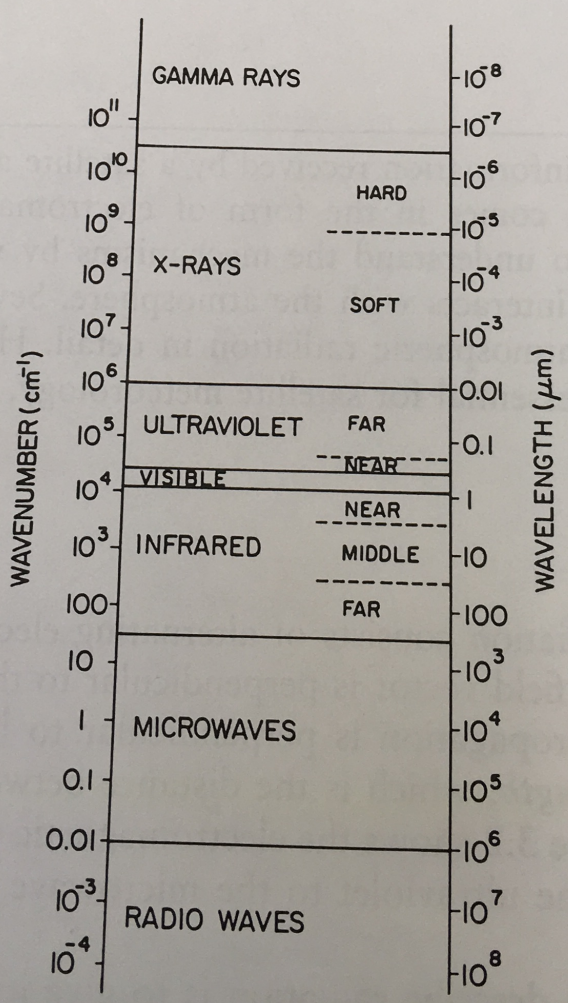

FIGURE 3.2. The electromagnetic spectrum.

TABLE 3.1. Radiation Symbols[a] and Units

Quantity	Recommended symbol	SI Unit
Frequency	ν	Hz
Wavelength	λ	m
Wavenumber	κ	m^{-1}
Radiant energy	Q	J
Radiant exposure	H	$J\ m^{-2}$
Radiant flux	Φ	W
Radiant flux density	M,E	$W\ m^{-2}$
Radiant exitance	M	$W\ m^{-2}$
Irradiance	E	$W\ m^{-2}$
Radiance	L	$W\ m^{-2}\ sr^{-1}$
Emittance	ε	Unitless
Absorptance	α	Unitless
Reflectance	ρ	Unitless
Transmittance	τ	Unitless
Absorption coefficient	σ_a	m^{-1}
Scattering coefficient	σ_s	m^{-1}
Extinction coefficient	σ_e	m^{-1}
Single-scatter albedo	$\tilde{\omega}$	Unitless
Absorption number	$\tilde{\alpha}$	Unitless
Vertical optical depth	δ	Unitless
Slant-path optical depth	δ_{sl}	Unitless
Scattering angle	ψ_s	rad
Scattering phase function	$p(\psi_s)$	sr^{-1}
Bidirectional reflectance	γ_r	sr^{-1}
Anisotropic reflectance factor	ξ_r	Unitless
Albedo	A	Unitless

[a] We use primarily the radiation symbols recommended by the Radiation Commission of the International Association of Meteorology and Atmospheric Sciences (IAMAS) as described in Raschke (1978).

most purposes, therefore, the speed of light in a vacuum can be safely used even in the atmosphere. However, strong vertical gradients of atmospheric density and humidity result in strong vertical gradients of n (see Section 3.5.3). These cause bending of electromagnetic rays and can cause slight mislocation of satellite scan spots.

One also sees radiation specified by *wavenumber*, κ, which is the reciprocal of the wavelength. Traditionally, wavenumber is expressed in inverse centimeters. Radiation with a 15-μm wavelength has a 667-cm^{-1} wavenumber, for example. Since wavenumber is inversely proportional to wavelength, it is directly proportional to frequency.

A fundamental property of electromagnetic radiation is that it can transport energy. Many of the units used to quantify electromagnetic radiation are based on energy.[1] These units are summarized in Table 3.1. The basic unit of *radiant*

[1] Some units, such as the lumen and the candela, are based on how bright an object appears to the human eye. These units are no longer used in satellite meteorology.

energy is the joule. *Radiant flux* is radiant energy per unit time, measured in watts [W; joules per second (J s^{-1})]. Radiant flux depends on area, which is often inconvenient; it is usually normalized by surface area. *Radiant flux density* is radiant flux crossing a unit area. It is measured, of course, in watts per square meter (W m^{-2}). Radiant flux density is so frequently used that it is subdivided to indicate which way the energy is traveling. *Radiant exitance* (M) is radiant flux density emerging from an area, and *irradiance* (E) is radiant flux density incident on an area.

In nature, radiation is a function of direction. The directional dependence is taken into account by employing the *solid angle*. If one draws lines from the center of the unit sphere to every point on the surface of an object, the area of the projection on the unit sphere is the solid angle (Fig. 3.3). The solid angle of an object that completely surrounds a point is 4π steradians (sr), the area of the unit sphere. The solid angle subtended by an infinite plane is 2π sr. For an object with cross-sectional area A_c at a distance r from a point ($A_c \ll r^2$), the solid angle is A_c/r^2. Solid angle is traditionally represented by the symbol Ω. If θ represents the zenith angle (the angle measured from the vertical or from the normal to a surface), and ϕ represents the azimuth angle (Fig. 3.4), then a differential element of solid angle is mathematically given by

$$d\Omega = \sin\theta d\theta d\phi = d\mu d\phi, \tag{3.2}$$

where $\mu \equiv \cos\theta$.

Radiant flux density per unit solid angle is known as *radiance* and is preferably assigned the symbol L. Suppose that a small element of surface is emitting radiation with radiance L. A question that arises is: What is the radiant exitance, that is, what is the total amount of radiation leaving the surface? This question is answered by integrating the radiance over the 2π sr above the surface. However, radiance represents the radiation leaving (or incident on) an area *perpendicular* to the beam. For other directions, we must weight the radiance by $\cos\theta$. Therefore, the

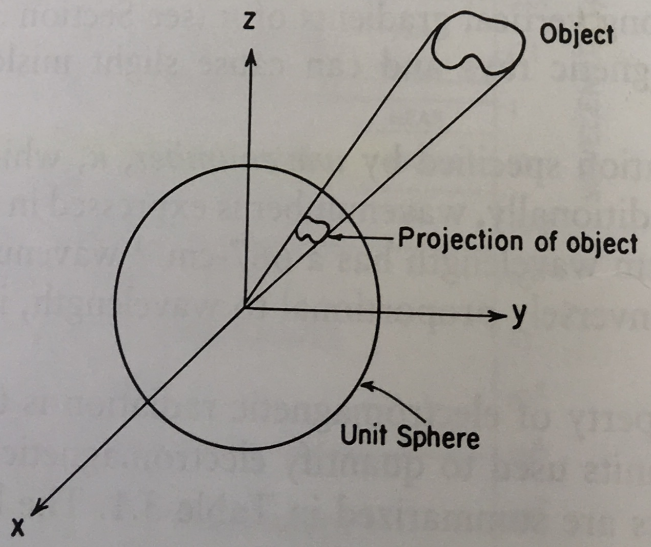

FIGURE 3.3. Illustration of a solid angle.

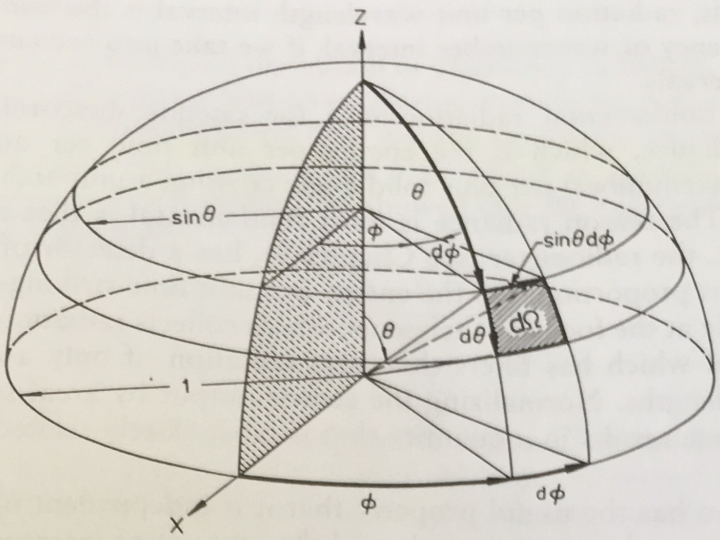

FIGURE 3.4. Mathematical representation of a solid angle. [After Raschke (1978), with permission of the International Association of Meteorology and Atmospheric Sciences.]

radiant exitance is

$$M = \int_0^{2\pi} L(\theta,\phi)\cos\theta\, d\Omega = \int_0^{2\pi}\int_0^{\pi/2} L(\theta,\phi)\cos\theta\sin\theta\, d\theta\, d\phi \qquad (3.3)$$

$$= \int_0^{2\pi}\int_0^{1} L(\mu,\phi)\,\mu\, d\mu\, d\phi$$

If the radiance is independent of direction (*isotropic*), then

$$M = L\int_0^{2\pi}\int_0^{\pi/2} \cos\theta\sin\theta\, d\theta\, d\phi = \pi L. \qquad (3.4)$$

The above energy-based quantities may all be prefixed with the word *monochromatic* or *spectral* to indicate the wavelength dependence of the radiation. A subscript (λ, ν, or κ) is used to indicate whether wavelength, frequency, or wavenumber is being considered. Because radiance is simply the integral over all wavelengths (frequencies, wavenumbers) of monochromatic radiance, we must have

$$L = \int_0^{\infty} L_\lambda d\lambda = \int_0^{\infty} L_\nu d\nu = \int_0^{\infty} L_\kappa d\kappa \qquad (3.5)$$

or

$$L_\lambda = -\frac{d\nu}{d\lambda} L_\nu = \frac{\nu^2}{c} L_\nu = \kappa^2 L_\kappa. \qquad (3.6)$$

In other words, radiation per unit wavelength interval is the same as radiation per unit frequency or wavenumber interval, if we take into account the different size of the intervals.

The most fundamental radiation unit for satellite meteorology is monochromatic radiance, which is the energy per unit time per unit wavelength (frequency, wavenumber) per unit solid angle crossing a unit area perpendicular to the beam. The reason radiance is most fundamental is that the basic satellite instrument, the radiometer (see Chapter 4), has a detector of a certain area whose output is proportional to the energy per unit time striking it. Further, the sensor is usually at the focus of a telescope which collects radiation from a certain solid angle and which has filters that pass radiation of only a certain narrow range of wavelengths. Normalizing the sensor output by area, solid angle, and wavelength range results in a quantity that is most closely related to monochromatic radiance.

Radiance also has the useful property that it is independent of distance from an object as long as the viewing angle and the amount of intervening matter are not changed. Consider a satellite viewing a small object. The irradiance reaching the satellite from the object will decrease inversely as the square of the distance of the satellite. However, the solid angle of the object subtended at the satellite will also decrease inversely as the square of the distance of the satellite. The radiance of the object as viewed by the satellite, which is simply the irradiance divided by the solid angle, is, therefore, independent of distance. Of course, if the object were at the Earth's surface, its radiance measured at the Earth's surface would be different from that measured at the satellite, due to the intervening atmosphere.

3.2 BLACKBODY RADIATION

All material above absolute zero in temperature emits radiation. Explaining the nature of this radiation was one of the chief problems facing physicists in the nineteenth century. As usual, though, nature guards her secrets. If one looks at two different kinds of material, each at the same temperature, one finds that the radiation being emitted by them is different. This led physicists to invent the perfect emitter, known as a *blackbody*, which emits the maximum amount of radiation at each wavelength. Although some materials come very close to being perfect emitters in some wavelength ranges, no real material is a perfect blackbody. Fortunately, the radiation inside a cavity whose walls are thick enough to prevent any radiation from passing directly through them can be shown to be the radiation that would be emitted by a blackbody. By observing the radiation inside cavities (through small holes) physicists knew, by the late nineteenth century, the empirical relationship between blackbody radiation and the two variables on which it depends: temperature and wavelength.

3.2.1 The Planck Function

In searching for a theoretical derivation of blackbody radiation, Planck[2] made the revolutionary assumption that an oscillating atom in the wall of a cavity can exchange energy with the radiation field inside a cavity only in discrete bundles called *quanta* given by $\Delta E = h\nu$, where h is known as *Planck's constant* (see Appendix E). With this assumption, he showed that the radiance being emitted by a blackbody is given by

$$B_\lambda(T) = \frac{2hc^2\lambda^{-5}}{\exp\left(\frac{hc}{\lambda kT}\right) - 1}, \tag{3.7}$$

where k is Boltzmann's[3] constant (see Appendix E), and T is the absolute temperature. Equation 3.7 is known as the *Planck function*; it earned him the Nobel Prize in 1918. The Planck function is more conveniently written as

$$B_\lambda(T) = \frac{c_1\lambda^{-5}}{\exp\left(\frac{c_2}{\lambda T}\right) - 1}, \tag{3.8}$$

where c_1 and c_2 are the first and second radiation constants (see Appendix E). Since the radiance from a blackbody is independent of direction, the radiant exitance from a blackbody is simply πB_λ.

Figure 3.5 shows $B_\lambda(T)$ plotted versus wavelength and temperature. It is important to note that $B_\lambda(T)$ is a monotonically increasing function of T. For a particular wavelength $\lambda = \Lambda$, if T_1 is less than T_2, then $B_\Lambda(T_1)$ is less than $B_\Lambda(T_2)$. $B_\lambda(T)$ is not monotonic in λ. For any temperature T, $B_\lambda(T)$ has a single maximum at a wavelength that may be determined by setting the partial derivative of $B_\lambda(T)$ with respect to λ equal to zero. The result is known as *Wein's[4] displacement law:*

$$\lambda_m T = 2897.9\ \mu\text{m K}, \tag{3.9}$$

where λ_m is the wavelength (expressed in micrometers) of maximum emission for a blackbody at temperature T (expressed in kelvins). Wein's displacement law was discovered empirically; he was awarded the Nobel Prize for it in 1911. The dashed line in Fig. 3.5 shows this relationship.

Another important aspect of the Planck function is its integral over wavelength. The total radiant exitance from a blackbody is

$$M_{BB} = \int_0^\infty \pi B_\lambda(T)\,d\lambda = \frac{\pi^5}{15} c_1 c_2^{-4} T^4 = \sigma T^4, \tag{3.10}$$

[2] Max Karl Ernst Ludwig Planck, German physicist, 1858–1947.
[3] Ludwig Eduard Boltzmann, Austrian physicist, 1844–1906.
[4] Wilhelm Wein, German physicist, 1864–1928.

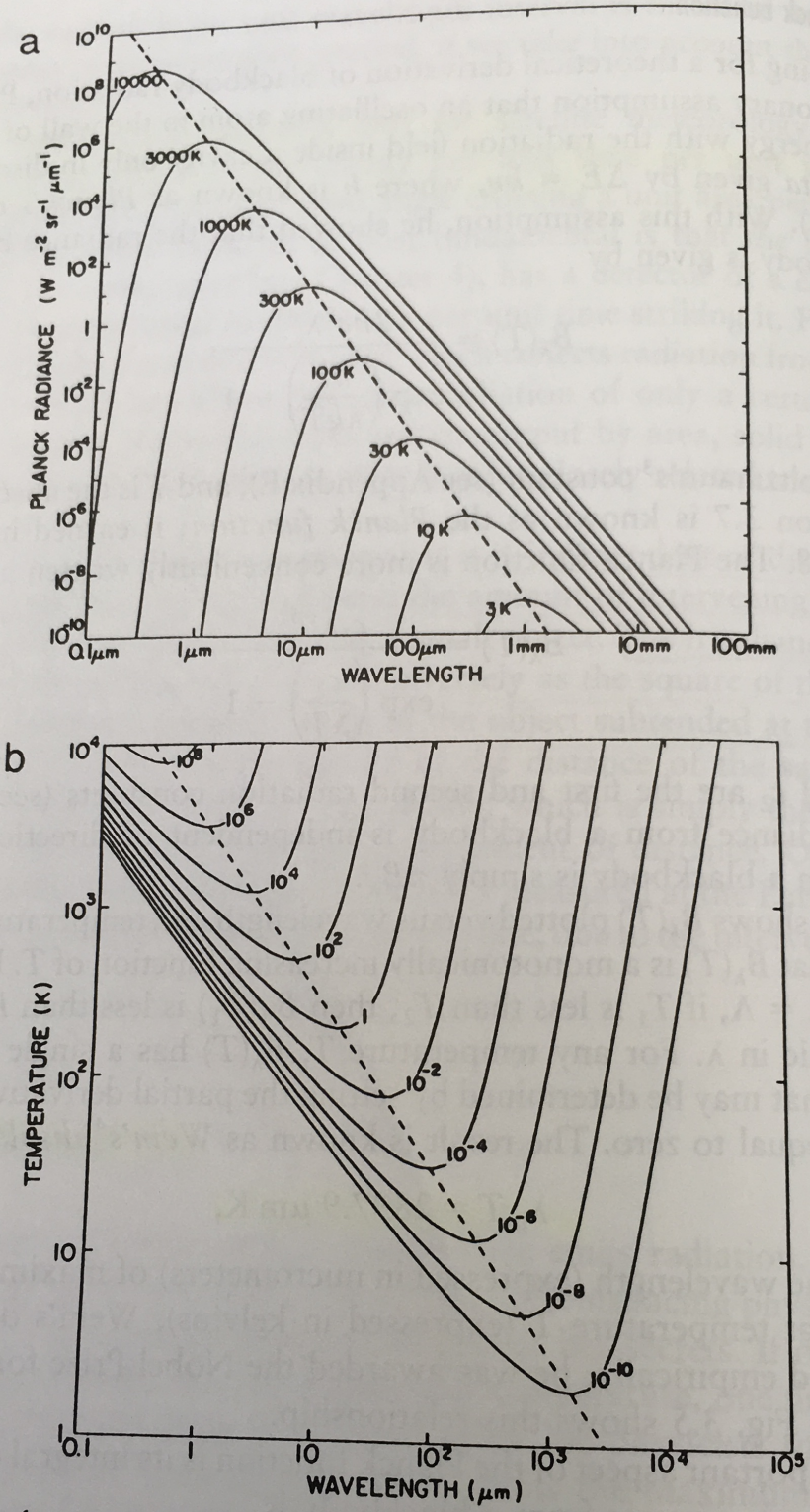

FIGURE 3.5. The Planck function. (a) Planck radiance versus wavelength for the indicated temperature, (b) temperature versus wavelength for the indicated Planck radiances (W $m^{-2}sr^{-1}\mu m^{-1}$), (c) Planck radiance versus temperature for the indicated wavelengths. The dashed line is Wein's displacement law, which gives the wavelength of maximum emission as a function of temperature.

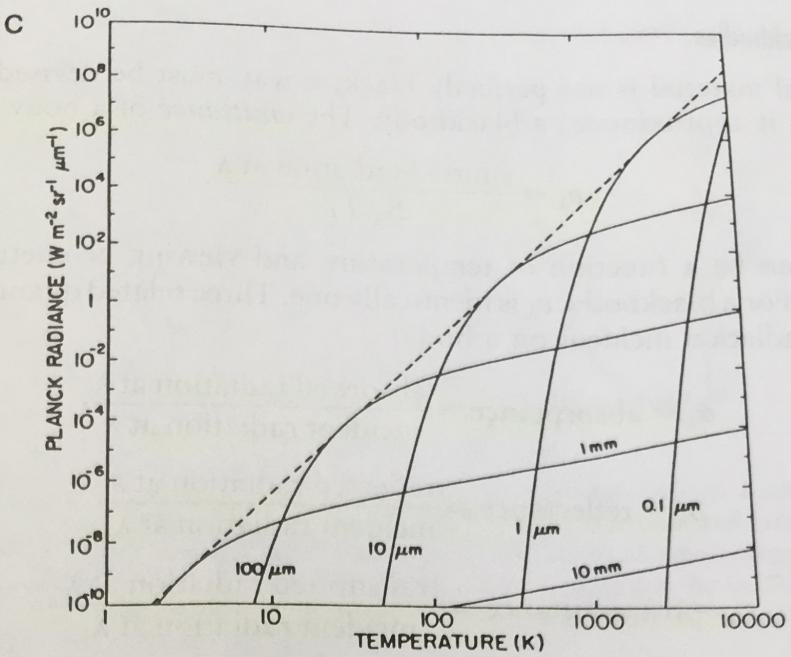

FIGURE 3.5. (*continued*)

where σ is called the *Stefan–Boltzmann constant* (see Appendix E), and Eq. 3.10 is called the *Stefan–Boltzmann law*.[5]

Finally, we would like to discuss a useful approximation to the Planck function. At millimeter and centimeter wavelengths, for temperatures encountered on the Earth and in its atmosphere, $c_2/\lambda T \ll 1$. Thus $\exp(c_2/\lambda T)$ can be approximated by $1 + c_2/\lambda T$. The Planck function then becomes

$$B_\lambda(T) = \frac{c_1}{c_2}\lambda^{-4}T. \tag{3.11}$$

This is known as the *Rayleigh–Jeans*[6] *approximation*. It says that in the microwave portion of the spectrum, radiance is simply proportional to temperature. In fact, in the microwave region, it is customary to divide radiance values by $(c_1/c_2)\lambda^{-4}$ and to refer to the quotient as *brightness temperature*. Brightness temperature is also used in the infrared portion of the spectrum, where it is known as *equivalent blackbody temperature*. However, equivalent blackbody temperature must be found by inverting the Planck function rather than by simple division.

[5] Named after Josef Stefan, Austrian physicist, 1835–1893, who discovered it by observing the cooling rates of hot bodies; and Boltzmann, who demonstrated it using thermodynamics.

[6] After John William Strutt, 3rd Baron Rayleigh, English physicist, 1842–1919; and Sir James Hopwood Jeans, English mathematician and astronomer, 1877–1946.

3.2.2 Nonblackbodies

Since real material is not perfectly black, a way must be devised to quantify how closely it approximates a blackbody. The *emittance* of a body is defined as

$$\varepsilon_\lambda \equiv \frac{\text{emitted radiation at } \lambda}{B_\lambda(T)}. \tag{3.12}$$

Emittance can be a function of temperature and viewing geometry as well as wavelength. For a blackbody, ε_λ is identically one. Three related quantities describe the fate of radiation incident on a body:

$$\alpha_\lambda = \text{absorptance} \equiv \frac{\text{absorbed radiation at } \lambda}{\text{incident radiation at } \lambda}, \tag{3.13a}$$

$$\rho_\lambda = \text{reflectance} \equiv \frac{\text{reflected radiation at } \lambda}{\text{incident radiation at } \lambda}, \tag{3.13b}$$

$$\tau_\lambda = \text{transmittance} \equiv \frac{\text{transmitted radiation at } \lambda}{\text{incident radiation at } \lambda}. \tag{3.13c}$$

Because these three processes are the only possibilities for the incident radiation,[7] by energy conservation, each quantity must be between zero and one, and

$$\alpha_\lambda + \rho_\lambda + \tau_\lambda \equiv 1. \tag{3.14}$$

Kirchhoff[8] discovered that a body is exactly as good an absorber as it is an emitter.[9] This is summarized in *Kirchhoff's law:*

$$\alpha_\lambda \equiv \varepsilon_\lambda. \tag{3.15}$$

This law applies only to material that is in *local thermodynamic equilibrium*, which means that it can be characterized by a single thermodynamic temperature. This is a good assumption below about 100 km in the Earth's atmosphere. Above 100 km, collisions between molecules are rare enough that different chemical species can have different thermodynamic temperatures. For most satellite meteorology applications, however, the Earth's atmosphere can be considered to be in local thermodynamic equilibrium.

Since the emittance of a blackbody is by definition one, its absorptance must also be one; that is, a blackbody, in addition to being a perfect emitter, is also a perfect absorber. It therefore appears black, thus the name *blackbody*.

The emittance of real materials is enormously variable. Shown in Fig. 3.6 is the emittance of two materials used in the Suomi radiometer discussed in Chapter 1. The black paint is supposed to approximate a blackbody by absorbing all radiation incident on it. Anodized aluminum looks like flat white paint. It is supposed to reflect solar radiation and absorb infrared radiation emitted by the

[7] We will not consider Raman scattering or fluorescence, in which radiation is absorbed at one wavelength and reemitted at another.

[8] Gustav Robert Kirchhoff, German physicist, 1824–1887.

[9] Assuming the contrary can be shown to violate the second law of thermodynamics.

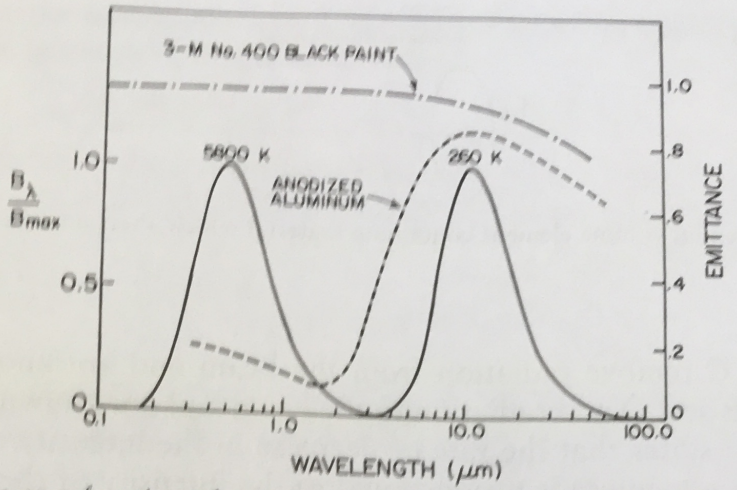

FIGURE 3.6. Emittance as a function of wavelength for two materials used in a satellite radiometer. Normalized Planck curves representing solar radiation (5800 K) and terrestrial radiation (260 K) are shown. (Do not be deceived by these normalized curves. The sun's radiance is larger than the Earth's at every wavelength.) [Adapted from Smith, W. L. (1985). Satellites. In D. D. Houghton (ed.), *Handbook of Applied Meteorology*. Copyright © 1985, John Wiley & Sons, Inc. Reprinted by permission of John Wiley & Sons, Inc.]

Earth and its atmosphere (*terrestrial radiation*). The difference between measurements made with instruments coated with these materials is related to the amount of incident solar radiation.

3.3 THE RADIATIVE TRANSFER EQUATION

At last we are ready to discuss the transfer of electromagnetic radiation through the atmosphere. Consider radiation incident on a differential volume of atmosphere (or, more generally, material) shown in Fig. 3.7. The equation that will be developed deals with the change in radiance as the radiation passes through the volume. Radiance is the appropriate variable because, as explained above, if there were no material in the volume, the radiance would not change.

If we do not consider polarization effects, four processes can change the radiance as it passes through the volume:

A. Radiation from the beam can be absorbed by the material.
B. Radiation can be emitted by the material.
C. Radiation can be scattered out of the beam into other directions.
D. Radiation from other directions can be scattered into the beam.

The rate of change of radiance with distance, dL_λ/ds, then consists of the above four terms:

$$\frac{dL_\lambda}{ds} = A + B + C + D. \tag{3.16}$$

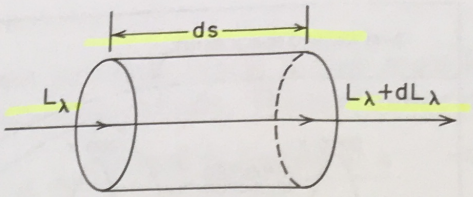

FIGURE 3.7. Differential volume element containing material which alters a beam of radiation passing through it.

Terms *A* and *C* remove radiation from the beam and are known as *depletion terms*. Terms *B* and *D* add radiation to the beam and are known as *source terms*.

Beer's law[10] states that the rate of decrease in the intensity of radiation as it passes through a medium is proportional to the intensity of the radiation. Term *A*, therefore, takes the form $-\sigma_a(\lambda)L_\lambda$, where $\sigma_a(\lambda)$ is the *volume absorption coefficient* and is equal to $\rho\beta_a(\lambda)$, where ρ is the density of absorber and $\beta_a(\lambda)$ is the *mass absorption coefficient*.[11] If Beer's law is integrated over a finite depth of absorber from *a* to *b*, then

$$L_\lambda = L_o \exp\left(-\int_a^b \sigma_a(\lambda)\,ds\right), \tag{3.17}$$

where *s* is distance along the path and L_o is the radiance incident on the absorber. If there were no scattering, the transmittance (Eq. 3.13c) would be

$$\tau_\lambda(a,b) = \exp\left(-\int_a^b \sigma_a(\lambda)\,ds\right), \tag{3.18}$$

and the absorptance (Eq. 3.13a) would be $1 - \tau_\lambda$.

The emission with which we will be concerned is Planckian emission. Since by Kirchhoff's law a material is as good an emitter as an absorber, term *B* takes the form $+\sigma_a(\lambda)B_\lambda(T)$.

Scattering of radiation out of the beam follows Beer's law. Term *C* takes the form $-\sigma_s(\lambda)L_\lambda$, where $\sigma_s(\lambda)$ is the *volume scattering coefficient*.

Finally, Term *D* describes the amount of radiation from other directions that is scattered into the beam. This term is complicated by the fact that all directions must be considered. If we are concerned with radiation traveling in a direction specified by the angles θ and ϕ, then Term *D* is given by

$$\text{Term } D = +\frac{\sigma_s(\lambda)}{4\pi}\int_0^{2\pi}\int_0^{\pi} L_\lambda(\theta',\phi')\,p(\psi_s)\sin\theta'\,d\theta'\,d\phi', \tag{3.19}$$

[10] After Wilhelm Beer, German astronomer, 1779–1850. It is also known as *Bouguer's law*, after the French mathematician Pierre Bouguer (1698–1758), who first published it in 1729; and as *Lambert's law*, after the German mathematician Johann Heinrich Lambert (1728–1777).

[11] σ_a has SI units of m^{-1} (reciprocal meters); ρ, of course, has SI units of kg m^{-3}; and β_a has SI units of m^2 kg^{-1}.

where (θ',ϕ') represents the direction of incoming radiation, and ψ_s is the *scattering angle* (the angle between θ, ϕ and θ', ϕ'):

$$\cos\psi_s = \cos\theta\cos\theta' + \sin\theta\sin\theta'\cos(\phi - \phi'). \tag{3.20}$$

$p(\psi_s)$ is called the *scattering phase function*. Basically, it tells what portion of the radiation from direction (θ',ϕ') is scattered into direction (θ,ϕ). $p(\psi_s)$ has the property that

$$\frac{1}{4\pi}\int_0^{2\pi}\int_0^{\pi} p(\psi_s)\sin\theta'\,d\theta'\,d\phi' \equiv 1. \tag{3.21}$$

(For an isotropic scatterer, $p(\psi_s) \equiv 1$.) Term D can be thought of as the product of $\sigma_s(\lambda)$ and a directionally weighted average [$p(\psi_s)$ is the weight] of the radiance from all directions:

$$\text{Term } D = \sigma_s(\lambda)\langle L'_\lambda\rangle, \tag{3.22}$$

where

$$\langle L'_\lambda\rangle \equiv \frac{1}{4\pi}\int_0^{2\pi}\int_0^{\pi} L_\lambda(\theta',\phi')\,p(\psi_s)\sin\theta'\,d\theta'\,d\phi'. \tag{3.23}$$

Combining all terms, the *radiative transfer equation* for nonpolarized radiation[12] becomes

$$\frac{dL_\lambda}{ds} = -\sigma_a(\lambda)L_\lambda(\theta,\phi) - \sigma_s(\lambda)L_\lambda(\theta,\phi) + \sigma_a(\lambda)B_\lambda(T) + \frac{\sigma_s(\lambda)}{4\pi}\int_0^{2\pi}\int_0^{\pi} L_\lambda(\theta',\phi')\,p(\psi_s)\sin\theta'\,d\theta'\,d\phi'. \tag{3.24}$$

This is a very complex equation. It is useful to examine its physical meaning before attempting to solve it.

Substituting Eq. 3.23 and rearranging slightly, the radiative transfer equation becomes

$$\frac{dL_\lambda}{ds} = \sigma_a(\lambda)[B_\lambda(T) - L_\lambda(\theta,\phi)] + \sigma_s(\lambda)[\langle L'_\lambda\rangle - L_\lambda(\theta,\phi)]. \tag{3.25}$$

Consider a beam of radiation upwelling through a thin atmospheric layer on its way to a satellite. The first term on the right-hand side of Eq. 3.25 represents the effects of absorption and emission. If $\sigma_a(\lambda)$ is zero, the layer is transparent absorptionally, and the beam passes through it unchanged. If $\sigma_a(\lambda)$ is not zero, the temperature of the layer and the radiance itself determine the change in the beam. The beam is augmented if $B_\lambda(T)$ is greater than $L_\lambda(\theta,\phi)$; it is diminished if $B_\lambda(T)$ is less than $L_\Lambda(\theta,\phi)$. The second term on the right represents the effects

[12] The radiative transfer equation for polarized radiation is not much more complicated. Polarized radiation can be described by a vector whose elements are the four Stokes parameters. The scattering phase function becomes a 4 × 4 matrix. The reader is referred to Liou (1980) for further details.

of scattering. If scattering particles are absent, $\sigma_s(\lambda)$ is zero, and scattering has no effect on the beam. If $\sigma_s(\lambda)$ is nonzero, the beam is augmented if the directionally weighted average radiance $\langle L'_\lambda \rangle$ is greater than the beam radiance $L_\lambda(\theta,\phi)$; it is diminished if $\langle L'_\lambda \rangle$ is less than $L_\lambda(\theta,\phi)$.

The radiative transfer equation can be formally solved. Since we will not use the formal solution, we refer readers to Goody and Yung (1989) for further discussion of it. Instead, we will concentrate on several simplifications that are used in satellite meteorology.

The first two terms on the right-hand side of Eq. 3.24 can be combined to form $-\sigma_e(\lambda)L_\lambda(\theta,\phi)$, where

$$\sigma_e(\lambda) \equiv \sigma_a(\lambda) + \sigma_s(\lambda) \tag{3.26}$$

is called the *volume extinction coefficient.*

It is convenient to divide the radiative transfer equation by the extinction coefficient and to introduce a new variable, δ_{sl}, the *slant path optical depth*:

$$\delta_{sl}(s_1,s_2) \equiv \int_{s_1}^{s_2} \sigma_e(\lambda,s)\,ds. \tag{3.27}$$

Because most meteorological variables are known as a function of height z rather than of slant path s (Fig. 3.8), we will use the *vertical optical depth*

$$\delta_\lambda(z_1,z_2) \equiv \int_{z_1}^{z_2} \sigma_e(\lambda,z)\,dz. \tag{3.28}$$

Since the Earth's atmosphere is thin in comparison with the radius of the Earth, the two optical depths are related by

$$\delta_{sl}(s_1,s_2) = \frac{\delta_\lambda(z_1,z_2)}{\mu}, \tag{3.29}$$

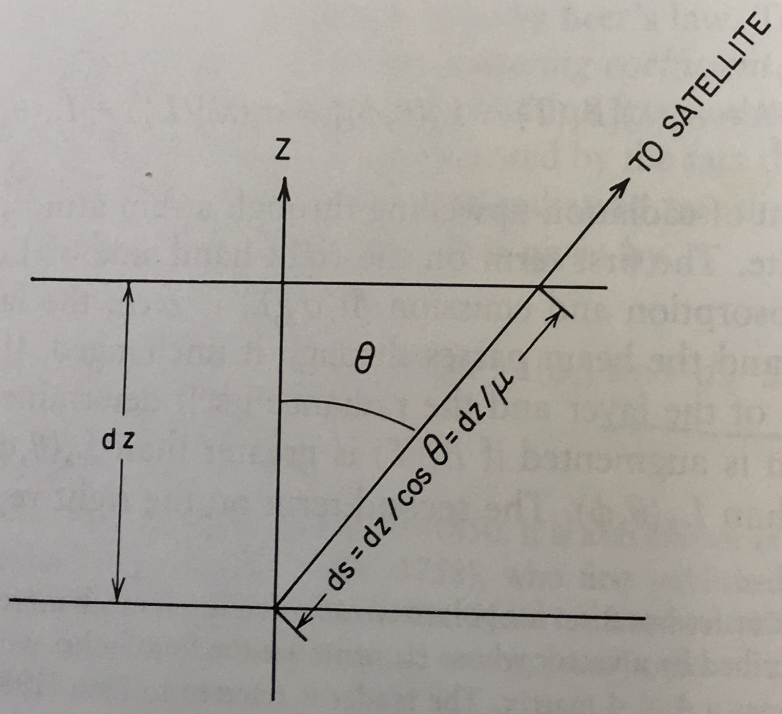

FIGURE 3.8. Relationship of depth to slant path through an infinitesimal atmospheric slab.

where μ is the cosine of the zenith angle θ, z_1 corresponds to s_1, and z_2 corresponds to s_2. We will use the symbol δ_λ without arguments to mean the vertical optical depth between the surface and level z, that is, $\delta_\lambda = \delta_\lambda(0,z)$, and therefore, $d\delta_\lambda = \sigma_e dz = \mu\sigma_e ds$.

Two additional definitions are useful. The *absorption number*, $\tilde{\alpha}_\lambda$, is defined as

$$\tilde{\alpha}_\lambda \equiv \frac{\sigma_a(\lambda)}{\sigma_e(\lambda)}, \tag{3.30}$$

and the *single-scatter albedo*, $\tilde{\omega}_\lambda$, is defined as

$$\tilde{\omega}_\lambda \equiv \frac{\sigma_s(\lambda)}{\sigma_e(\lambda)}. \tag{3.31}$$

With these definitions, the radiative transfer equation becomes

$$\mu \frac{dL_\lambda}{d\delta_\lambda} = -L_\lambda(\theta,\phi) + \tilde{\alpha}_\lambda B_\lambda(T) + \frac{\tilde{\omega}_\lambda}{4\pi}\int_0^{2\pi}\int_{-1}^{1} L_\lambda(\mu',\phi')\, p(\psi_s)\, d\mu'\, d\phi'. \tag{3.32}$$

Note that we have substituted μ for $\cos\theta$ in this equation, as is commonly done.

Now we are ready to simplify and solve the radiative transfer equation. We will explore two common simplifications: the no-scattering case and the no-emission case.

3.3.1 No-Scattering Equations

A common assumption is that scattering is negligible. This is a good assumption in the infrared portion of the spectrum in the absence of clouds. If there is no scattering, the single-scatter albedo is zero, and the absorption number is one. The radiative transfer equation then becomes

$$\mu \frac{dL_\lambda}{d\delta_\lambda} = -L_\lambda(\theta,\phi) + B_\lambda(T), \tag{3.33}$$

which is known as *Schwarzchild's equation*.[13]

The infrared radiance observed by a satellite (in the absence of scattering) can be calculated by formally integrating Schwarzchild's equation. Since Schwarzchild's equation is a first-order, linear, ordinary differential equation, its integration is straightforward. A detailed derivation is justified, however, because the result is arguably the most important equation in satellite meteorology. To start, we rearrange Eq. 3.33 and multiply by the integrating factor $\exp(\delta_\lambda/\mu)/\mu$:

$$\exp\left(\frac{\delta_\lambda}{\mu}\right)\frac{dL_\lambda}{d\delta_\lambda} + \frac{1}{\mu}\exp\left(\frac{\delta_\lambda}{\mu}\right)L_\lambda(\theta,\phi) = \frac{1}{\mu}\exp\left(\frac{\delta_\lambda}{\mu}\right)B_\lambda(T). \tag{3.34}$$

The left-hand side is now an exact differential:

$$\frac{d}{d\delta_\lambda}\left[\exp\left(\frac{\delta_\lambda}{\mu}\right)L_\lambda(\theta,\phi)\right] = \frac{1}{\mu}\exp\left(\frac{\delta_\lambda}{\mu}\right)B_\lambda(T). \tag{3.35}$$

[13] After Karl Schwarzchild, German astronomer, 1873–1916.

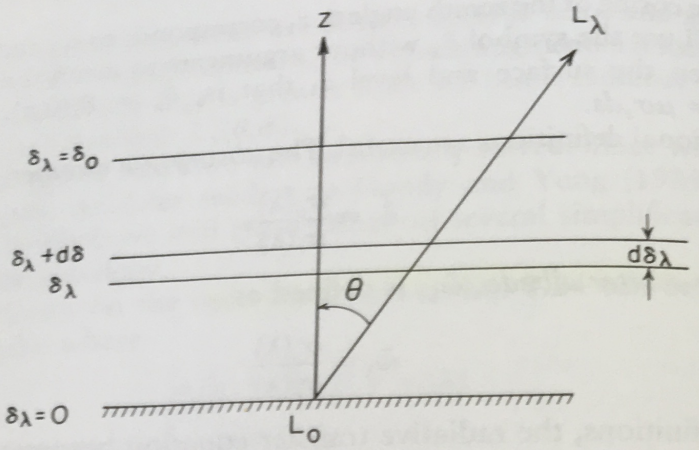

FIGURE 3.9. The vertical optical depth coordinate system.

Using δ_λ as the vertical coordinate (Fig. 3.9), Eq. 3.35 can be integrated from the Earth's surface ($\delta_\lambda = 0$) to the satellite ($\delta_\lambda = \delta_o$):[14]

$$\int_0^{\delta_o} \frac{d}{d\delta_\lambda}\left[\exp\left(\frac{\delta_\lambda}{\mu}\right) L_\lambda(\theta,\phi)\right] d\delta_\lambda = \int_0^{\delta_o} \exp\left(\frac{\delta_\lambda}{\mu}\right) B_\lambda(T)\,\frac{d\delta_\lambda}{\mu}. \tag{3.36}$$

Because the left-hand side of Eq. 3.36 is the integral of an exact differential, the integral is simply

$$\left[\exp\left(\frac{\delta_\lambda}{\mu}\right) L_\lambda\right]_0^{\delta_o} = \exp\left(\frac{\delta_o}{\mu}\right) L_\lambda - L_o = \int_0^{\delta_o} \exp\left(\frac{\delta_\lambda}{\mu}\right) B_\lambda(T)\,\frac{d\delta_\lambda}{\mu}, \tag{3.37}$$

where L_λ is the radiance reaching the satellite, and L_o is the radiance leaving the surface. Solving for L_λ:

$$L_\lambda = L_o \exp\left(-\frac{\delta_o}{\mu}\right) + \int_0^{\delta_o} \exp\left(-\frac{(\delta_o - \delta_\lambda)}{\mu}\right) B_\lambda(T)\,\frac{d\delta_\lambda}{\mu}. \tag{3.38}$$

This equation forms the basis for sounding the atmosphere and for corrections necessary for surface parameter estimation (Chapter 6).

The vertical transmittance (see Section 3.2.2) of the atmospheric layer between optical depths δ_1 and δ_2 is

$$\tau_\lambda(\delta_1,\delta_2) \equiv \exp(-|\delta_2 - \delta_1|). \tag{3.39}$$

We will use the symbol τ_λ without arguments to mean the vertical transmittance of the layer between level δ_λ and the satellite (δ_o),[15] that is, $\tau_\lambda \equiv \tau_\lambda(\delta_\lambda,\delta_o)$. The

[14] Meteorological satellites orbit well above the effective top of the atmosphere; therefore, δ_o is the vertical optical depth of the entire atmosphere.

[15] This definition is a little unusual. The customary definition is $\tau_\lambda \equiv \exp(-\delta_\lambda)$. However, this transmittance is that between the surface and level δ_λ. Since the transmittance between δ_λ and δ_o is a much more useful quantity, we adopt $\tau_\lambda \equiv \exp[-(\delta_o - \delta_\lambda)]$.

transmittance between the surface and the satellite is $\tau_o = \tau_\lambda(0,\delta_o)$. With the aid of these definitions, the integrated form of Schwarzchild's equation has a simple physical explanation.

Equation 3.38 says that the radiance reaching a satellite comes from two sources. The first term on the right-hand side is the surface term. L_o is the radiance leaving the surface; $\exp(-\delta_o/\mu) = \tau_o^{1/\mu}$ is the transmittance of the entire atmosphere along the slant path to the satellite. The product is that portion of the surface radiance which reaches the satellite. The second term is the contribution of the atmosphere. Since we are not considering scattering,

$$\frac{d\delta_\lambda}{\mu} = \sigma_a \frac{dz}{\mu}, \tag{3.40}$$

that is, $d\delta_\lambda/\mu$ is the emittance of the atmospheric layer between δ_λ and $\delta_\lambda + d\delta_\lambda$. Therefore, $B_\lambda(T)\,d\delta_\lambda/\mu$ is the radiance emitted in the direction of the satellite by the layer. The factor $\exp[-(\delta_o - \delta_\lambda)/\mu] = \tau_\lambda^{1/\mu}$ is the slant path transmittance from δ_λ to the satellite. Therefore, the product $\exp[-(\delta_o - \delta_\lambda)/\mu]B_\lambda(T)\,d\delta_\lambda/\mu$ is that portion of the radiance emitted by the atmospheric layer between δ_λ and $\delta_\lambda + d\delta_\lambda$ which reaches the satellite. The integral indicates that the contributions of all atmospheric layers are to be summed.

A useful rule of thumb is that a satellite receives the maximum radiation from the layer which is one optical depth into the atmosphere, that is, where $(\delta_o - \delta_\lambda)/\mu = 1$. This rule is exact for the uninteresting case of an isothermal atmosphere and is approximately correct for other atmospheres.

Note that it is sometimes convenient to use transmittance as the vertical coordinate:

$$L_\lambda = L_o\tau_o^{1/\mu} + \int_{\tau_o}^{1} B_\lambda(T)\,\tau_\lambda^{(1/\mu-1)}\,\frac{d\tau_\lambda}{\mu}. \tag{3.41}$$

For overhead viewing ($\mu = 1$),

$$L_\lambda = L_o\tau_o + \int_{\tau_o}^{1} B_\lambda(T)\,d\tau_\lambda. \tag{3.42}$$

3.3.2 No-Emission Equations

Neither the Earth nor its atmosphere emits significant radiation at visible or near-infrared wavelengths. For these wavelengths, Planck emission $[B_\lambda(T)]$ may be neglected, and the radiative transfer equation becomes

$$\mu\frac{dL_\lambda}{d\delta_\lambda} = -L_\lambda(\mu,\phi) + \frac{\tilde{\omega}_\lambda}{4\pi}\int_0^{2\pi}\int_{-1}^{1} L_\lambda(\mu',\phi')\,p(\psi_s)\,d\mu'\,d\phi'. \tag{3.43}$$

Neither liquid water nor water vapor absorbs much radiation in the visible portion of the spectrum. At visible wavelengths, it is often acceptable to assume that absorption in clouds is zero, or equivalently that $\tilde{\omega}_\lambda = 1$. This approximation is called *conservative scattering* because radiative energy is conserved: all of the

energy that is incident on a cloud is assumed to emerge from it, although in various directions.

The source of ultraviolet, visible, and near-infrared radiation is, of course, the sun. It is convenient and traditional to divide this radiation into *direct-beam radiation*, which comes directly from the sun without any interaction with the atmosphere, and *diffuse radiation*, which has undergone at least one scattering event in the atmosphere or reflection from the surface. Direct-beam radiation follows Beer's law:

$$L_\lambda^{\text{direct}} = L_\lambda^{\text{sun}} \exp\left(-\frac{\delta_o - \delta_\lambda}{\mu_{\text{sun}}}\right), \tag{3.44}$$

where L_λ^{sun} is the sun's radiance at the top of the atmosphere, and μ_{sun} is the cosine of the solar zenith angle. The diffuse radiation is described by Eq. 3.43, but one correction must be made. When the second term of Eq. 3.43 is calculated, both direct and diffuse radiation must be considered. Since the sun's radiation comes from essentially only one direction $(\theta_{\text{sun}},\phi_{\text{sun}})$, the direct-beam term can be taken out of the integral, leaving only the diffuse radiance:

$$\mu \frac{dL_\lambda^{\text{diffuse}}}{d\delta_\lambda} = -L_\lambda^{\text{diffuse}}(\mu,\phi) + \frac{\tilde{\omega}_\lambda}{4\pi}\int_0^{2\pi}\int_{-1}^{1} L_\lambda^{\text{diffuse}}(\mu',\phi')\, p(\psi_s)\, d\mu'\, d\phi'$$

$$+ \frac{\tilde{\omega}_\lambda}{4\pi} L_\lambda^{\text{sun}} \Omega_{\text{sun}} \exp\left(-\frac{\delta_o - \delta_\lambda}{\mu_{\text{sun}}}\right) p(\psi_{\text{sun}}), \tag{3.45}$$

where Ω_{sun} is the solid angle subtended by the sun, and ψ_{sun} is the scattering angle between the sun and the observed direction (θ,ϕ). The product $L_\lambda^{\text{sun}}\Omega_{\text{sun}}$ is the solar spectral irradiance, E_λ^{sun}. Equation 3.45 is used to study clouds' effects on radiation. It includes the multiple scattering of radiation that occurs in thick clouds, and it has challenged atmospheric scientists for many years. The reader is referred to Liou (1980) for a discussion of the ways it has been approached.

A further approximation, which is useful for the study of aerosols (see Chapter 8) and thin clouds, is that only the first scattering need be considered. This is called the *single-scattering approximation*, and it is equivalent to neglecting the second term in Eq. 3.45, which deals with the scattering of diffuse (already scattered) radiation.

In order to apply the radiative transfer equation, we must have a knowledge of the absorption and scattering properties of the Earth's atmosphere, the reflection properties of the Earth's surface, and the characteristics of the sun's radiation. These will be dealt with in the next four sections.

3.4 GASEOUS ABSORPTION

The study of absorption and emission by gases is the field of spectroscopy, an old and complex science which was largely explained by quantum mechanics in the first half of the twentieth century (Herzberg, 1950; McCartney, 1983). Radia-

tion can interact with atmospheric gases in five ways: ionization–dissociation interactions, electronic transitions, vibrational transitions, rotational transitions, and forbidden transitions.

3.4.1 Radiative Interactions

In *ionization–dissociation interactions*, an electron is stripped from an atom or molecule, or a molecule is torn apart. These interactions occur primarily at ultraviolet and shorter wavelengths. Because any energy greater than the threshold energy will ionize or dissociate a molecule, these interactions produce relatively smooth *spectra* (plots of absorption coefficient versus wavelength or wavenumber), unlike the spectra produced by the processes described below.

If one divides the absorption coefficient by the number density (number of molecules per unit volume), one arrives at a quantity with the units of area that spectroscopists call the *absorption cross section*. It is a molecule's effective area, that is, a measure of how effectively it absorbs radiation. Figure 3.10 shows a semischematic representation of the absorption cross sections of O_3, O_2, and N_2 in the ultraviolet and visible portions of the spectrum.

All solar radiation shorter than about 0.1 μm in wavelength is absorbed in the upper atmosphere by ionizing atmospheric gases, particularly atomic oxygen; this ionization produces the ionosphere. Wavelengths between 0.1 and 0.2 μm are absorbed by dissociation of molecular oxygen (O_2) into atomic oxygen. Short of about 0.2423 μm, O_2 dissociates in the Herzberg continuum. Short of about

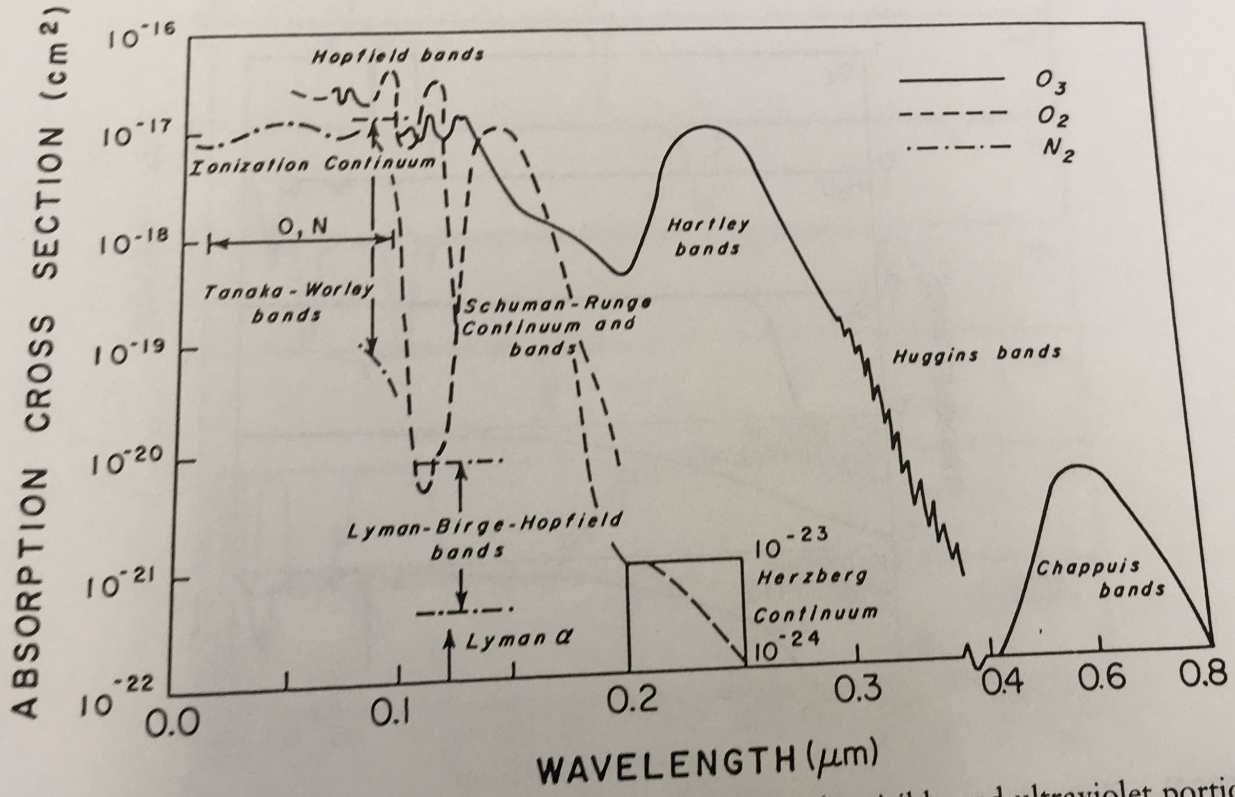

FIGURE 3.10. Absorption cross sections of atmospheric gases in the visible and ultraviolet portions of the spectrum. Note that these curves are intended to indicate the relative significance of various absorbers and should not be taken as the source of quantitative data. [After Liou (1980). Reprinted by permission of Academic Press.]

0.1750 μm, O_2 dissociates in the much stronger Schuman–Runge continuum. Virtually all radiation between 0.2 and 0.3 μm is absorbed by dissociation of ozone (O_3) in the Hartley bands. Ozone also dissociates in the weak Chappuis bands in the visible portion of the spectrum. Ionization–dissociation interactions are important to satellite meteorology primarily for measuring ozone concentration profiles.

In *electronic transitions*, an orbital electron jumps between quantized energy levels. These transitions occur mostly in the ultraviolet and visible portions of the spectrum. Of importance to satellite meteorology are the ultraviolet Huggins bands of ozone, which are used to measure integrated (total) ozone, and a weak 0.77-μm band (the A band) of molecular oxygen, which may someday be used to estimate surface pressure by measuring the total amount of O_2 in an atmospheric column. Figure 3.11 shows the vertical transmittance of the Earth's atmosphere in the visible, ultraviolet, and near-infrared portions of the spectrum.

In *vibrational transitions*, a molecule changes vibrational energy states. These transitions occur mostly in the infrared portion of the spectrum and are extremely important for satellite meteorology. They are discussed in the next section. At temperatures found in the Earth's atmosphere, most molecules are in the ground vibrational state. The spectrum of vibrational transitions, therefore, is caused primarily by transitions between the ground state and the first vibrational excited state.

In *rotational transitions*, a molecule changes rotational energy states. These occur in the far-infrared and microwave portion of the spectrum. However, rota-

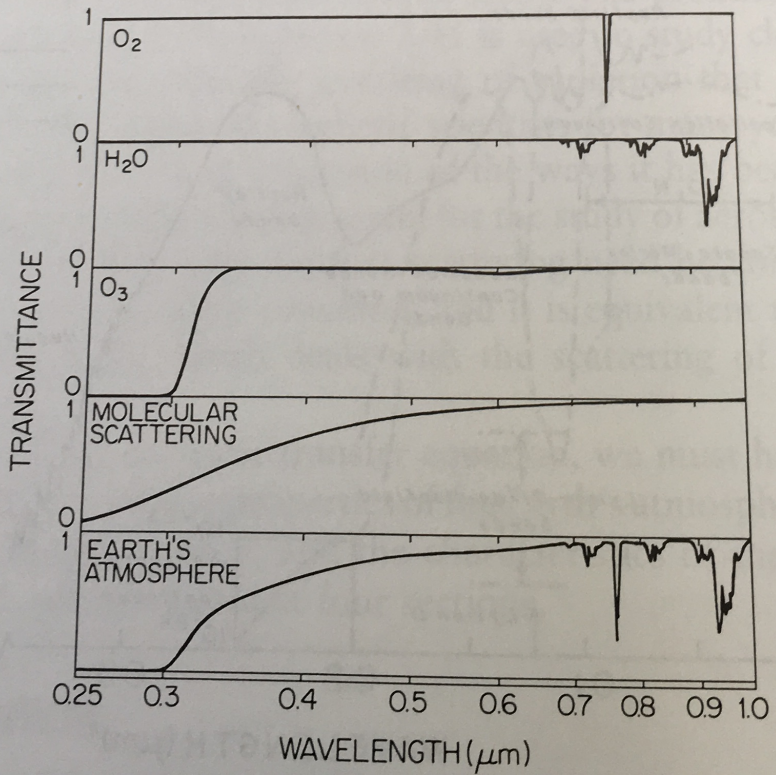

FIGURE 3.11. Vertical transmittance of the Earth's atmosphere between 0.25 and 1.0 μm. Rayleigh scattering by air molecules is the chief limitation to the transfer of visible radiation through the clear atmosphere. The effects of aerosols have not been included in these curves. [Calculated using LOWTRAN 6 (Kneizys *et al.*, 1983).]

tional transitions can occur at the same time as a vibrational transition, which complicates the spectrum. Figure 3.12 shows the infrared spectrum of the radiatively most important atmospheric gases. The far-infrared spectrum is dominated by rotational transitions of water vapor. Measurement of water vapor in the microwave region is an important use of rotational transitions.

Finally, *forbidden transitions* are those transitions which are not caused by the interaction between the electric field of the radiation and the electric dipole moment of a molecule. Some forbidden transitions do, in fact, occur. A meteorologically important forbidden transition is caused by the reorientation of unpaired electron spins in the O_2 molecule. This results in an absorption band in the 5-mm region which is used for temperature sounding. Figure 3.13 shows the microwave spectrum of the Earth's atmosphere.

Figure 3.14 shows the complete spectrum of the Earth's atmosphere under very low spectral resolution. Although much of the spectrum is opaque because of absorption by atmospheric gases, there are several important areas, called *windows*, where the atmosphere is relatively (but *not* absolutely) transparent. The most important of these are the visible window, the 3.7-μm window, the microwave windows (2–4 mm and >6 mm), and the 8.5–12.5 μm window. This

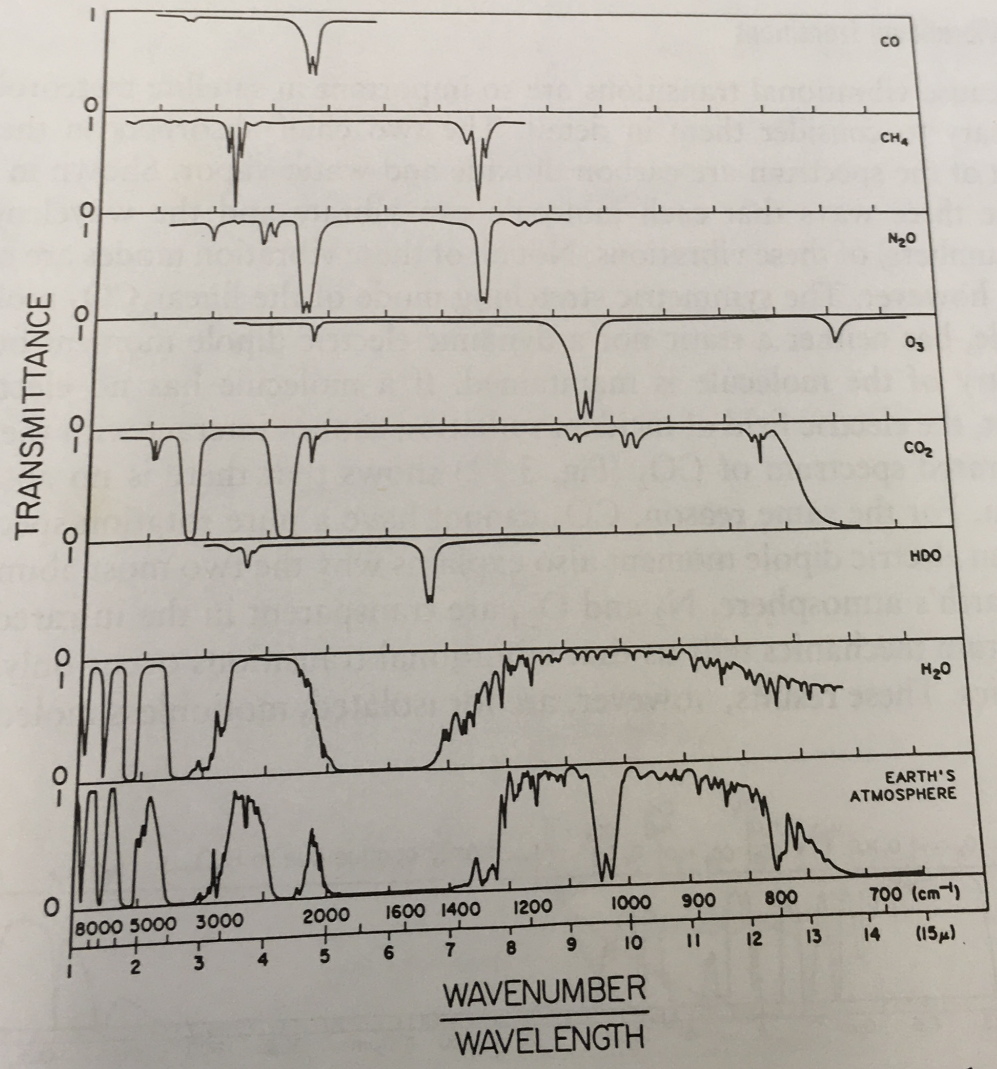

FIGURE 3.12. Infrared transmittance of several gases in the Earth's atmosphere and the combined atmospheric transmittance. [After Valley (1965).]

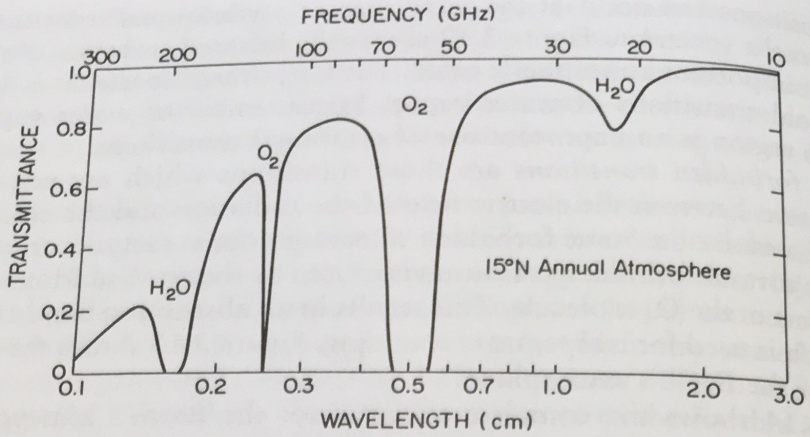

FIGURE 3.13. Transmittance of the Earth's atmosphere in the microwave portion of the spectrum. [Calculated using the model of Liebe and Gimmestad (1978).]

last window is punctuated by the 9.6-μm ozone absorption band (vibrational), and it is affected by water vapor absorption.

3.4.2 Vibrational Transitions

Because vibrational transitions are so important in satellite meteorology, it is necessary to consider them in detail. The two chief absorbers in the infrared region of the spectrum are carbon dioxide and water vapor. Shown in Fig. 3.15 are the three ways that each molecule can vibrate and the wavelengths (and wavenumbers) of these vibrations. Not all of these vibration modes are radiatively active, however. The symmetric stretching mode of the linear CO_2 molecule, for example, has neither a static nor a dynamic electric dipole moment because the symmetry of the molecule is maintained. If a molecule has no electric dipole moment, the electric field of incident radiation cannot interact with the molecule. The infrared spectrum of CO_2 (Fig. 3.12) shows that there is no absorption at 7.46 μm. For the same reason, CO_2 cannot have a pure rotation spectrum. The lack of an electric dipole moment also explains why the two most abundant gases in the Earth's atmosphere, N_2 and O_2, are transparent in the infrared.

Quantum mechanics tells us that vibrational transitions occur only at discrete frequencies. These results, however, are for isolated, motionless molecules. In the

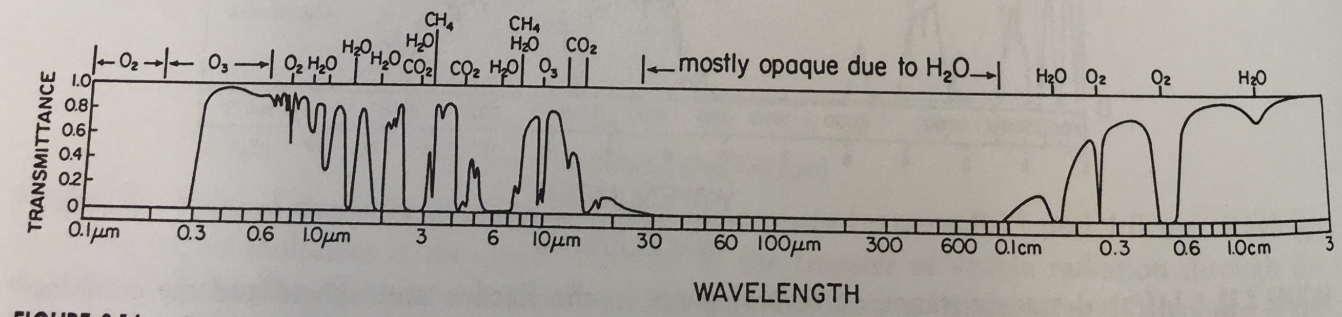

FIGURE 3.14. Spectrum of the Earth's atmosphere. [Adapted from Goody and Yung (1989), with permission from Oxford University Press.]

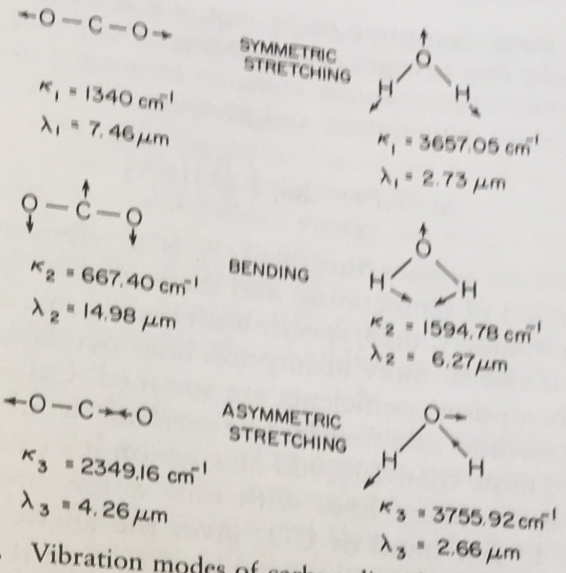

FIGURE 3.15. Vibration modes of carbon dioxide and water vapor.

Earth's atmosphere, absorption lines are broadened chiefly by collisions, which distort the molecule and cause it to absorb (or emit) at slightly different wavelengths. Infrared lines are usually modeled as having the *Lorentz lineshape* (Fig. 3.16):

$$\beta_a(\kappa) = \frac{(\Delta\kappa)S}{\pi[(\kappa - \kappa_0)^2 + (\Delta\kappa)^2]}, \tag{3.46}$$

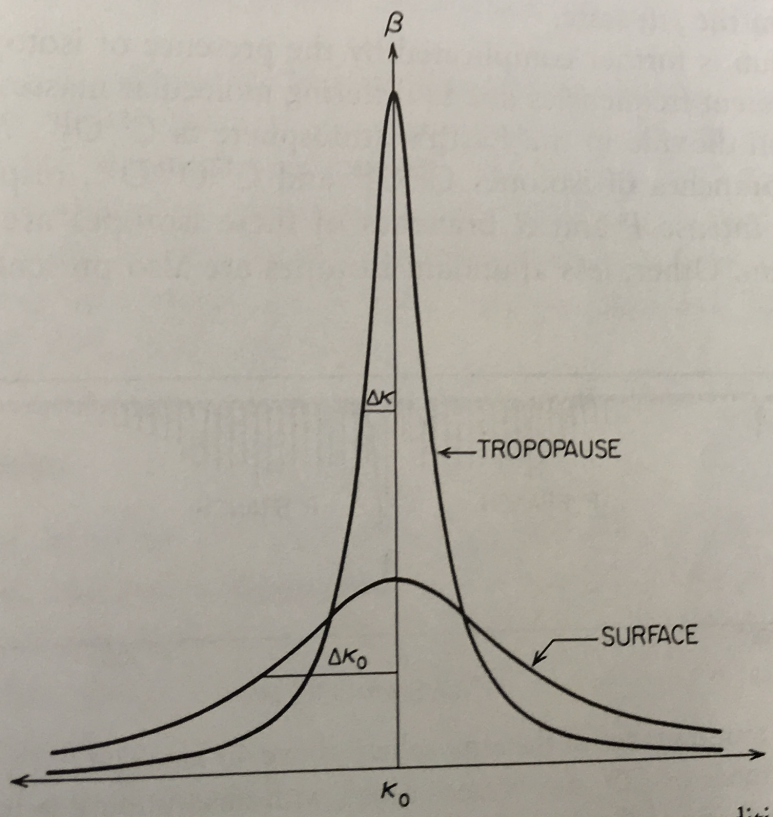

FIGURE 3.16. The Lorentz lineshape for near-surface and near-tropopause conditions; κ_0 is the central wavenumber, and $\Delta\kappa$ is the halfwidth, which is a function of temperature and pressure.

where $\beta_a(\kappa)$ is the mass absorption coefficient, κ is wavenumber, κ_o is the central wavenumber, S is the line strength (independent of $\Delta\kappa$), and $\Delta\kappa$ is the halfwidth. The halfwidth is proportional to the collision frequency of a molecule and can be shown to depend on temperature and pressure as

$$\Delta\kappa(T,P) = \Delta\kappa_o \left(\frac{P}{P_o}\right)\left(\frac{T_o}{T}\right)^{1/2}, \tag{3.47}$$

where T_o is a reference temperature, and P_o is a reference pressure. The line strength S is a function of temperature and the energy of the lower level (E'') of the transition. Four numbers, then, specify each line: κ_o, S_o, $\Delta\kappa_o$, and E'' (McClatchey *et al.*, 1973). If two or more absorption lines overlap, which is usually the case, the *volume* absorption coefficients are summed. Calculation of absorption coefficients by this method (the *line-by-line method*) would not be too difficult except that there are more than 100,000 absorption lines between 1 and 25 μm!

How can there be so many lines with only a few absorbing gases? Close examination of the 15-μm band of CO_2 gives the answer. Figure 3.17 shows what serves as a high-resolution spectrogram of CO_2 in the wavenumber range 600–740 cm^{-1} (16.67–13.51 μm). The bending mode vibrational transition occurs at 667.40 cm^{-1} (14.98 μm). Quantum-mechanical selection rules, however, allow rotational transitions to accompany vibrational transitions. The rotational quantum number J may change by +1, forming the higher frequency R *branch*; 0, forming the central Q *branch*; or −1, forming the lower frequency P *branch*. In addition, the energy of the Jth rotational state is proportional to $J(J+1)$. The difference between the J and $J+1$ energy levels is therefore linearly related to J. Since many excited rotational states are populated, the P and R branches consist of a series of equally spaced lines, the strengths of which are related to the number of molecules in the Jth state.

The spectrum is further complicated by the presence of isotopes that vibrate at slightly different frequencies due to differing molecular masses. The dominant form of carbon dioxide in the Earth's atmosphere is $C^{12}O_2^{16}$. At 649 and 662 cm^{-1}, the Q branches of isotopes $C^{13}O_2^{16}$ and $C^{12}O^{16}O^{18}$, respectively, can be seen. The less intense P and R branches of these isotopes are masked by the $C^{12}O_2^{16}$ spectrum. Other, less abundant isotopes are also present.

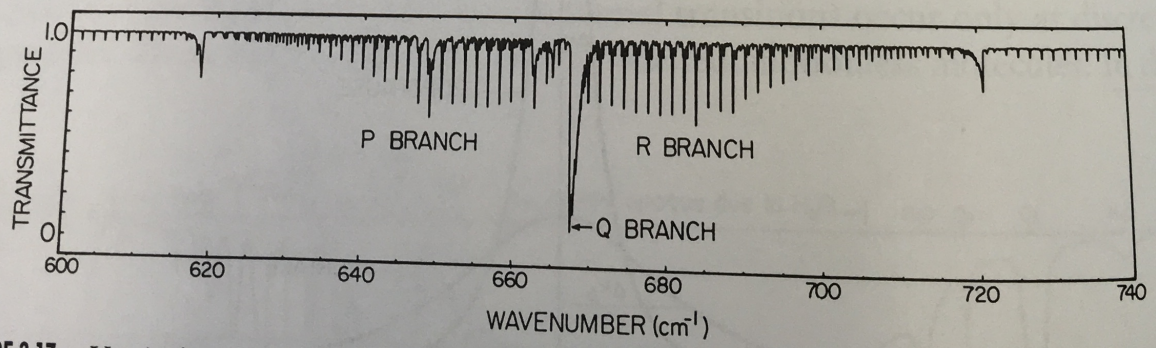

FIGURE 3.17. Vertical transmittance of the atmosphere above 40 km. The P, Q, and R branches of the bending vibrational mode of CO_2 can be seen along with absorption due to isotopes of CO_2 (see text). [Adapted from Kyle and Goldman (1975).]

The spectrum is still further complicated by combination and overtone bands. A *combination band* is one in which two transitions take place simultaneously. At 618 and 721 cm^{-1}, for example, one can see bands which arise from the transition of the symmetric stretching mode from the ground state to the first excited state simultaneous with the transition of the bending mode from the first excited state to the ground state. An *overtone band* is one in which a molecule absorbs (or emits) a photon of sufficient energy to cause it to jump two or more levels. Water vapor, for example, absorbs in a band centered at 3151 cm^{-1}, which is the result of double excitation of its bending mode. When all of these complications are taken into account, 100,000 is not an unreasonable number of absorption lines, even though only a handful of atmospheric gases contribute to the infrared spectrum.

Comparing Fig. 3.17 with Fig. 3.12, one might ask: Why are the rotational transitions not evident in Fig. 3.12? The answer has two parts. First, Fig. 3.12 shows the transmittance of the entire atmosphere. Near the surface, the individual rotation lines are considerably broadened (Fig. 3.16) so that they overlap each other. Second, Fig. 3.12 is what is called a *low-resolution spectrum*. The spectrum is averaged over a passband and therefore appears smooth. The result of these two effects is that in Fig. 3.12, only the envelopes of the *P*, *Q*, and *R* branches of absorption bands are discernable. Note also that not all molecules have a *Q* branch. Ozone, for example, has a bimodal absorption band centered at 9.6 μm, which consists of the envelope of its *P* and *R* branches.

A complete compilation of vibration–rotation lines important for satellite meteorology has been made by the U.S. Air Force Geophysics Laboratory (McClatchey *et al.*, 1973) and an optimized computer codes to calculate atmospheric transmittances have been written, for example, FASCOD (Clough *et al.*, 1982). Readers who need to do line-by-line calculations are advised to obtain one of these codes.

Vibrational transitions are the basis of temperature sounding and measurement of a wide variety of trace gases in the atmosphere. The 15-μm and 4.3-μm CO_2 bands are used for temperature sounding. The 6.3-μm H_2O band is used for water vapor measurements. The 9.6-μm band of ozone is used to make total ozone measurements. Several other important gases have been measured in the stratosphere using vibrational transitions. Among them are NO, N_2O, NO_2, HNO_3, HCl, HF, CH_4, CO, and CO_2.

3.4.3 Practical Problems

Two problems arise in the application of absorption line data in satellite meteorology. First, the parameters that specify absorption lines are not perfectly known. Calculated atmospheric transmittances agree with laboratory measurements only to within about 10%. This uncertainty results in errors in temperature retrievals, for example.

The second problem is that the radiative transfer equation is strictly only valid at a single wavelength. A typical satellite sounder channel, however, is about 20

cm^{-1} wide (see Chapter 4), which includes several lines. Calculation of the radiance that a satellite radiometer would measure requires the calculation of radiance at many closely spaced wavelengths followed by integration over the passband of the radiometer channel:

$$L_{\text{measured}} = \frac{\int_{\lambda_1}^{\lambda_2} L_\lambda f(\lambda)\, d\lambda}{\int_{\lambda_1}^{\lambda_2} f(\lambda)\, d\lambda}, \tag{3.48}$$

where $f(\lambda)$ is the response function of the radiometer channel. Even with fast line-by-line routines such as FASCOD, these calculations are too time consuming to be of practical use in many applications. Instead, one turns either to band models or to polynomial expansions.

In a *band model* the transmittance of an atmospheric layer in an entire band is calculated at one time using an appropriate parameterization, which is usually based on fitting line-by-line calculations to a function. Goody and Yung (1989, Chapter 4) explain several parameterizations. The LOWTRAN computer code (McClatchey *et al.*, 1972; Kneizys *et al.*, 1983), in which transmittance averaged over a 20-cm^{-1} band is calculated, is an example of this type of model.

In polynomial expansions, the atmosphere is divided into layers. For each layer and for each channel of the radiometer, transmittances are calculated line-by-line for a variety of temperatures and humidities. Polynomial functions of temperature and humidity are then fitted to the transmittances. To calculate the transmittance of the atmosphere from a particular level to a satellite, one uses an estimate of atmospheric temperature and humidity and calculates the transmittance of each layer. The total atmospheric transmittance is the product of the layer transmittances. Polynomial expansions are used extensively in satellite sounding (see McMillin and Fleming, 1976).

3.5 SCATTERING

Radiation scattered from a particle is a function of several things: particle shape, particle size, particle index of refraction, wavelength of radiation, and, of course, viewing geometry.[16] In 1908 Mie[17] applied Maxwell's[18] equations, which describe electromagnetic radiation, to the case of a plane electromagnetic wave incident on a sphere. The far-field radiation (that observed at many radii from the sphere) is the scattered radiation. [See Liou (1980) for this lengthy derivation.] Mie showed that for a spherical scatterer, the scattered radiation is a function of only viewing angle, index of refraction, and the *size parameter* defined as

$$\chi \equiv \frac{2\pi r}{\lambda}, \tag{3.49}$$

[16] See van de Hulst (1957) for a thorough discussion of scattering by particles.
[17] Gustav Mie, German physicist, 1868–1957.
[18] James Clerk Maxwell, Scottish mathematician and physicist, 1831–1879.

where r is the radius of the sphere. The size parameter can be used to divide scattering into three regimes (Fig. 3.18).

3.5.1 Mie Scattering

For size parameters in the range 0.1–50, the wavelength of the radiation and the circumference of the particle are comparable. Radiation strongly interacts with the particle, and, therefore, the full Mie equations must be used. These equations have been applied extensively to the detection of raindrops by radar. The study of aerosols (smoke, dust, haze) using visible radiation falls in the Mie regime. Also in the Mie regime is the interaction of cloud droplets with infrared radiation.

A complete discussion of Mie scattering is outside the scope of this book because the scattering equations are very complicated. Insight into the results, however, can be gained as follows. If the volume absorption coefficient is divided by the number of scattering particles per unit volume and by the cross-sectional area of each scatterer, the result is the *scattering efficiency* (Q_s) for a single scatterer. Q_s is the ratio of the total scattered radiation (regardless of direction) to the incident radiation. Q_s is a function of the size parameter and of the index of refraction of the particle.

Many substances absorb radiation as well as scatter it. This can be conveniently taken into account by letting the index of refraction become a complex number

$$m \equiv n - in', \tag{3.50}$$

where n, the real part of the index of refraction, is as defined above, and n', the imaginary part, accounts for absorption inside the scatterers. Figure 3.19 shows

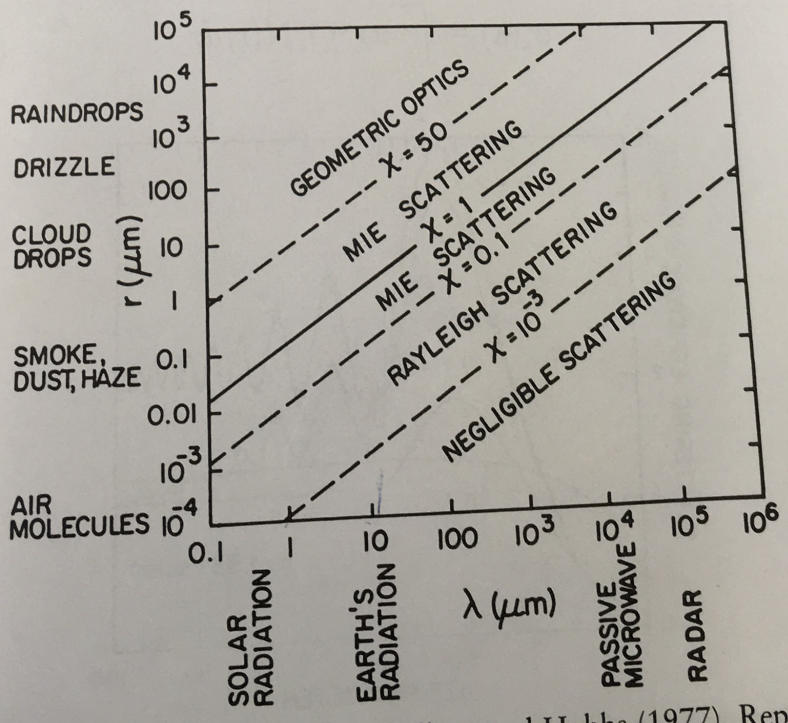

FIGURE 3.18. Scattering regimes. [Adapted from Wallace and Hobbs (1977). Reprinted by permission of Academic Press.]

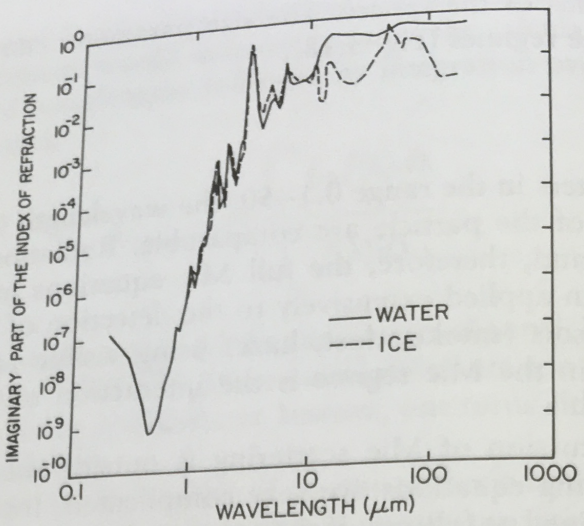

FIGURE 3.19. Imaginary part of the index of refraction of water and ice. [Plotted from data in Irvine and Pollack (1968).]

n' as a function of wavelength for water and ice. In the visible portion of the spectrum, n' is negligibly small, but in the infrared it becomes significant.

Figure 3.20 shows the scattering efficiency for water drops ($n = 1.33$) as a function of size parameter for several values of n'. Scattering efficiency in the Mie regime is quite clearly a complicated function. In clouds, there is usually a distribution of drop sizes. Suppose that $N(r)dr$ is the number of drops per unit volume in the radius range r to $r + dr$. If the scatterers are sufficiently far apart (many wavelengths) that they act independently, the scattering coefficient is given by

$$\sigma_s(\lambda) = \int_0^\infty \pi r^2 Q_s N(r) dr \tag{3.51}$$

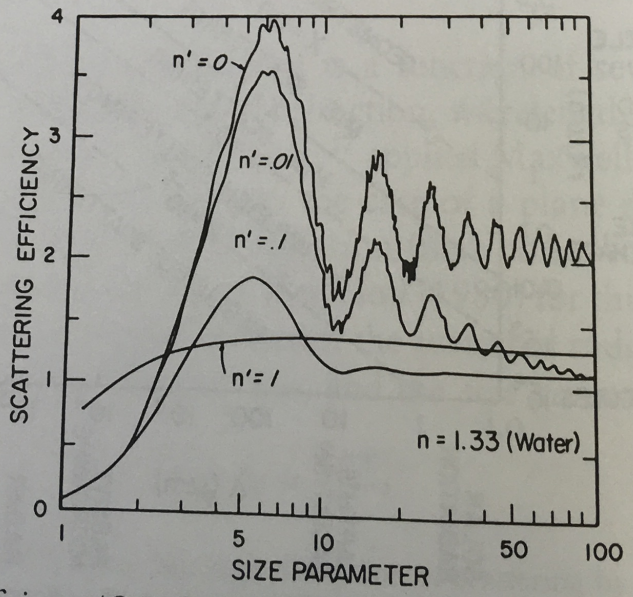

FIGURE 3.20. Scattering efficiency (Q_s) of water spheres ($n = 1.33$) as a function of size parameter (χ) for several values of n'. [Adapted from Liou (1980) and Hansen and Travis (1974). Reprinted by permission of Academic Press, Inc. and Kluwer Academic Publishers.]

Integration over the size distribution smooths the scattering efficiency. In any case, it must be noted that scattering is a much smoother function of wavelength than is gaseous absorption.

Also of interest is the scattering phase function, which determines in which direction the radiation is scattered. Figure 3.21 shows the scattering phase function for water drops for several size parameters. As the size parameter increases, the phase function becomes strongly peaked in the forward direction; relatively little radiation is backscattered toward the source of the radiation. Finally, we note that in general scattering polarizes radiation; in some applications polarization must be taken into account.

3.5.2 Geometric Optics

For χ greater than about 50, the sphere is large in comparison with the wavelength of radiation. This is the realm of *geometric optics*, where rays, which are reflected and refracted at the surface of a scatterer, can be traced. Ray tracing can be used with scatterers that are nonspherical. As shown in Fig. 3.18, the interaction of solar radiation with virtually all types of hydrometeors falls in this regime. A wide variety of optical phenomena such as rainbows and halos can be explained with geometric optics. The interaction of infrared radiation with precipitation-size particles also falls within this regime.

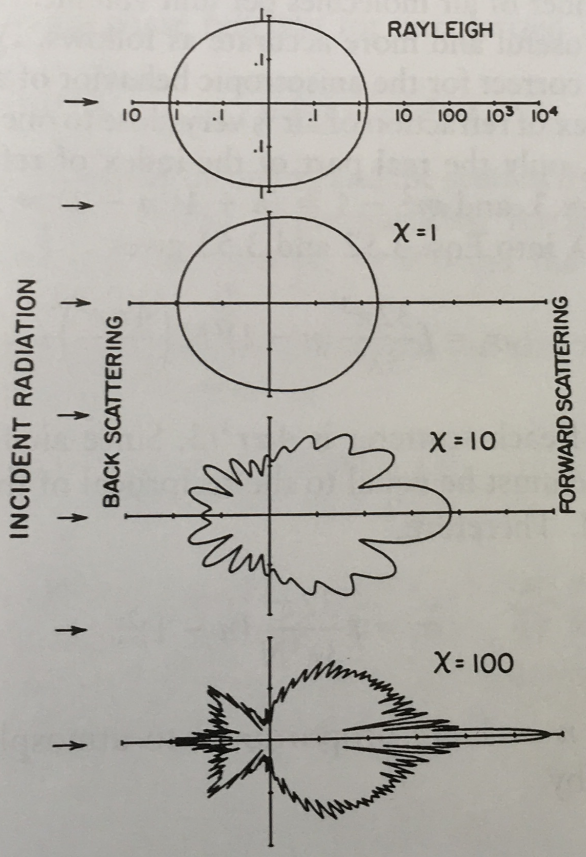

FIGURE 3.21. Polar plots (note the logarithmic scales) of the scattering phase function of water drops for several size parameters. [Plotted from data supplied by Steven A. Ackerman, Cooperative Institute for Meteorological Satellite Studies, University of Wisconsin–Madison.]

For nonabsorbing spheres, Fig. 3.20 shows that the scattering efficiency asymptotically approaches 2 as the size parameter increases. Not only is the radiation that directly strikes the drop scattered, but an equal amount of radiation that comes near the drop is *refracted* around it. Since the refracted radiation changes direction, it has been scattered.

3.5.3 Rayleigh Scattering

For χ less than about 0.1, only the first term in the Mie equations must be considered. The scattering efficiency becomes

$$Q_s = \frac{8\chi^4}{3}\left|\frac{m^2-1}{m^2+2}\right|^2, \tag{3.52}$$

where m is the complex index of refraction. Because the particle is small in comparison with the wavelength of the radiation, Rayleigh scattering is insensitive to particle shape; Eq. 3.52 works for nonspherical as well as spherical particles. Because of the χ^4 dependence, scattering becomes negligible for χ less than 10^{-3}.

Air molecules act as Rayleigh scatterers for visible and ultraviolet radiation. The scattering coefficient for air molecules should be simply

$$\sigma_s = \pi r^2 Q_s N, \tag{3.53}$$

where N is the number of air molecules per unit volume. However, this formula can be made more useful and more accurate as follows. First, we multiply by a factor $f = 1.061$ to correct for the anisotropic behavior of air molecules. Second, we note that the index of refraction of air is very close to one, and if only scattering is to be considered, only the real part of the index of refraction need be used. Therefore, $m^2 + 2 \approx 3$, and $m^2 - 1 = (n+1)(n-1) \approx 2(n-1)$. Substituting these and $\chi = 2\pi r/\lambda$ into Eqs. 3.52 and 3.53 gives

$$\sigma_s = f\frac{32\pi^3}{3\lambda^4}(n-1)^2 N\left(\frac{4\pi r^3}{3}\right)^2. \tag{3.54}$$

Third, the volume of each scatterer is $4\pi r^3/3$. Since air fills any volume that it occupies, this volume must be equal to the reciprocal of the number of scatterers per unit volume (N). Therefore,

$$\sigma_s = f\frac{32\pi^3}{3\lambda^4 N}(n-1)^2. \tag{3.55}$$

Finally, both N and $n - 1$ are proportional to atmospheric density ρ. For an ideal gas, N is given by

$$N = \left(\frac{N_A}{W_m}\right)\rho, \tag{3.56}$$

where N_A is Avogadro's[19] number (Appendix E), and W_m is the molecular weight of the gas (28.966 kg kmol^{-1} for dry air). The index of refraction of air is given by

$$n - 1 = \left(\frac{\rho}{\rho_o}\right)(n_o - 1), \tag{3.57}$$

where ρ_o and n_o are the sea-level values. The Rayleigh scattering coefficient for air then becomes

$$\sigma_s = f\frac{32\pi^3 W_m \rho}{3\rho_o^2 N_A \lambda^4}(n_o - 1)^2. \tag{3.58}$$

Liou (1980) states that $n_o - 1$ can be approximated as

$$(n_o - 1) \times 10^6 = 64.328 + \frac{29498.1}{146 - \lambda^{-2}} + \frac{255.4}{41 - \lambda^{-2}}, \tag{3.59}$$

where λ is in micrometers. Equation 3.58 states that for Rayleigh scattering, $\sigma_s(\lambda)$ is proportional to ρ, as it must be, and to the familiar λ^{-4}.

Figure 3.11 shows the vertical transmittance of the Earth's atmosphere due to Rayleigh (molecular) scattering. At visible and ultraviolet wavelengths, Rayleigh scattering by air molecules must be taken into account. Aerosol optical depth can be measured over the ocean *if* the observed radiance is corrected for Rayleigh scattering by air molecules (see Section 8.5). Rayleigh scattering of air molecules must also be taken into account when making ultraviolet measurements of ozone (see Section 6.5).

The Rayleigh scattering phase function for unpolarized incident radiation is given by

$$p_{\text{Rayleigh}}(\psi_s) = \tfrac{3}{4}(1 + \cos^2\psi_s), \tag{3.60}$$

where ψ_s is the angle between the incoming and the scattered radiation (Fig. 3.21). It is important to note that unlike larger particles, Rayleigh particles scatter equally well in the forward direction ($\psi_s = 0°$) and the backward direction ($\psi_s = 180°$).

Rayleigh particles, for example, cloud droplets, can also absorb radiation. The Rayleigh absorption efficiency is given by

$$Q_a = 4\chi I_m\left(\frac{m^2 - 1}{m^2 + 2}\right), \tag{3.61}$$

where I_m indicates the imaginary part. Because Q_a varies with χ while Q_s varies with χ^4, absorption can quickly dominate scattering for Rayleigh particles that have even the smallest amount of absorption. The absorption coefficient due to a number of particles is (similar to Eq. 3.51)

$$\sigma_a(\lambda) = \int_0^\infty \pi r^2 Q_a N(r)\,dr. \tag{3.62}$$

[19] Amedeo Avogadro, count of Quaregna, Italian physicist, 1776–1856.

In the Rayleigh regime, Q_a is proportional to r; thus $\sigma_a(\lambda)$ is proportional to the total volume of scatterer per unit volume of atmosphere. In a cloud, for example, absorption due to Rayleigh-size cloud droplets is proportional to the liquid water content. This is important in the microwave region where cloud droplets absorb, but do not scatter. Using microwave measurements, the vertically integrated liquid water content of clouds can be estimated (see Section 8.3).

3.5.4 Clouds

Because clouds play a large role in satellite meteorology, it is important to understand in a general way the interaction of clouds with radiation. Clouds consist of water drops or ice crystals with radii on the order of 10 μm. Drops with radii of 100 μm have significant fall speed and constitute drizzle. Drops with radii of 1000 μm (1 mm) are raindrops. Clouds have drop concentrations on the order of 10^8 m^{-3}; that is, the drops are on the order of 1 mm apart.

In the visible portion of the spectrum ($\lambda \sim 0.5$ μm), cloud drops are geometric scatterers; therefore, the scattering efficiency is approximately 2. The scattering coefficient, then, is ~0.1 m^{-1}. A photon's *mean free path* (the average distance between scattering events) is the reciprocal of the volume scattering coefficient, or ~10 m. Therefore, a cloud only a few tens of meters thick is sufficient to scatter all of the visible radiation incident on it. Since liquid water does not absorb visible radiation well, very little of the radiation is absorbed; most emerges from the cloud somewhere after being scattered many times. Welch *et al.* (1980), for example, have made calculations for a 2-km-thick stratus cloud with the sun directly over head (Table 3.2). At 0.55 μm, the cloud absorbs only 0.2% of incident radiation; 79.8% is scattered out the top of the cloud, and 20.0% is scattered out the bottom of the cloud. Since clouds have a distribution of drop sizes and the size parameter is large, all visible wavelengths are scattered nearly

TABLE 3.2. Calculated Radiative Properties of a 2-km-thick Stratus Cloud[a]

Wavelength (μm)	*Absorbed* (%)	*Scattered* (%)	
		Out top	*Out bottom*
0.55	0.2	79.8	20.0
0.765	0.5	80.6	18.9
0.95	8.1	76.3	15.5
1.15	17.9	70.4	11.7
1.4	47.4	49.9	2.7
1.8	61.9	37.6	0.5
2.8	99.6	0.4	0.0
3.35	99.4	0.6	0.0
6.6	99.05	0.95	0.0
Total	10.0	73.8	16.6

[a] From Table 2.12a of Welch *et al.* (1980).

equally well. Clouds therefore appear white. Solar radiation extends into the near infrared region of the spectrum. In the near infrared, absorption due to water vapor increases as does the absorption of liquid water. Averaged over the solar spectrum, Welch *et al.* (1980) calculate that the cloud absorbs 10.0%, scatters 73.8% out the top of the cloud, and scatters 16.2% out the bottom of the 2-km-thick cloud.

In the 8.5–12.5-μm window, cloud droplets are Mie scatterers. The scattering efficiency is roughly in the range 1–3, but in contrast to visible wavelengths, the absorption efficiency is on the order of 1. Therefore, clouds absorb nearly all of the infrared radiation incident on them. They act essentially as blackbodies.

In the microwave portion of the spectrum ($\chi \sim 0.01$), absorption due to cloud drops is very small. The transmittance of a typical nonraining cloud is greater than 90%. Scattering is negligibly small. Raindrop-size particles, however, interact strongly with microwave radiation. Therefore, clouds are nearly transparent in the microwave region, but raining clouds are not. This forms one basis of microwave detection of precipitation (see Chapter 9).

Cirrus clouds have a higher transmittance than water clouds because ice clouds have far fewer particles per unit volume than water clouds and because water is a better absorber than ice. Cirrus clouds can also be vertically thinner than water clouds. In general thin cirrus clouds are difficult to detect with satellite radiometers, yet their effects are not negligible. They can cause problems in the retrieval of atmospheric soundings (see Chapters 6 and 8). The detection of cirrus clouds with satellite instruments is an area of active research.

3.6 SURFACE REFLECTION

Reflected radiation, particularly reflected solar radiation and reflected microwave radiation, is very important to satellite meteorology. Several quantities are used to describe reflected radiation. The most basic is the *bidirectional reflectance*, γ_r, which is related to the fraction of radiation from incident direction (θ_i,ϕ_i) that is reflected in the direction (θ_r,ϕ_r). Perhaps the best way to define it is to write the formula for the radiance reflected from a small element of surface:

$$L_r(\theta_r,\phi_r) = \int_0^{2\pi}\int_0^{\pi/2} L_i(\theta_i,\phi_i)\,\gamma_r(\theta_r,\phi_r;\,\theta_i,\phi_i)\cos\theta_i \sin\theta_i\, d\theta_i\, d\phi_i. \qquad (3.63)$$

Basically, radiation from incident direction (θ_i,ϕ_i) illuminates a small element of surface. Taking into account the effect of incident angle, $L_i\cos\theta_i$ is available to be reflected. A fraction $\gamma_r(\theta_i,\phi_i;\,\theta_r,\phi_r)$ is reflected into direction (θ_r,ϕ_r). Integrating over all incident solid angles gives the reflected radiance in direction (θ_r,ϕ_r).

An important property of the bidirectional reflectance is known as the *Helmholtz reciprocity principle*. It states that the bidirectional reflectance is invariant if the directions of incoming and outgoing radiation are interchanged:

$$\gamma_r(\theta_r,\phi_r;\,\theta_i,\phi_i) = \gamma_r(\theta_i,\phi_i;\,\theta_r,\phi_r). \qquad (3.64)$$

Equation 3.64 is used in the construction of tables of bidirectional reflectance from satellite observations because not all incident radiation angles can be observed (see Chapter 10).

Probably the most frequently used reflection quantity is the *albedo* (A), which is the ratio of radiant exitance (M, due to reflection) to irradiance (E):

$$E = \int_0^{2\pi} \int_0^{\pi/2} L_i(\theta_i, \phi_i) \cos\theta_i \sin\theta_i \, d\theta_i \, d\phi_i, \tag{3.65a}$$

$$M = \int_0^{2\pi} \int_0^{\pi/2} L_r(\theta_r, \phi_r) \cos\theta_r \sin\theta_r \, d\theta_r \, d\phi_r, \tag{3.65b}$$

$$A \equiv \frac{M}{E}. \tag{3.65c}$$

Albedo is a unitless ratio between zero and one. As defined in Eqs. 3.65, it is a function of neither the incoming nor the outgoing angles; however, this does not mean that the albedo is constant. If the incoming radiation changes, the albedo will change. This is most easily understood by restricting the incoming radiation to direct-beam solar radiation, which comes from a very narrow range of angles. In this case,

$$E = L_{sun}\Omega_{sun} \cos\theta_{sun}, \tag{3.66a}$$

$$L_r(\theta_r, \phi_r) = L_{sun}\Omega_{sun} \cos\theta_{sun} \, \gamma_r(\theta_r, \phi_r; \theta_{sun}, \phi_{sun}), \tag{3.66b}$$

$$M = L_{sun}\Omega_{sun} \cos\theta_{sun} \int_0^{2\pi} \int_0^{\pi/2} \gamma_r(\theta_r, \phi_r; \theta_{sun}, \phi_{sun}) \cos\theta_r \sin\theta_r \, d\theta_r \, d\phi_r, \tag{3.66c}$$

$$A(\theta_{sun}, \phi_{sun}) = \frac{M}{E} = \int_0^{2\pi} \int_0^{\pi/2} \gamma_r(\theta_r, \phi_r; \theta_{sun}, \phi_{sun}) \cos\theta_r \sin\theta_r \, d\theta_r \, d\phi_r, \tag{3.66d}$$

where Ω_{sun} is the solid angle of the sun subtended at the Earth. Since the direction of the sun remains in the equation, the albedo is a function of solar direction.

As an example of reflecting surfaces, two limiting cases are useful. A *Lambertian* or *isotropic reflector* reflects radiation uniformly in all directions. If its albedo is A, then its bidirectional reflectance is a constant A/π. Flat white paint approximates a perfect ($A = 1$, independent of wavelength) Lambertian reflector. A *specular reflector* is like a mirror; its bidirectional reflectance is strongly peaked. Solar radiation from a perfect specular reflector would be observed only at the zenith angle equal to the solar zenith angle and at the azimuth angle equal to the solar azimuth angle plus 180°. Water surfaces are similar to specular reflectors, except that real water surfaces are always somewhat rough, so the solar reflection is blurred and larger than the sun. This is called *sun glint* or *sun glitter* (see Chapter 5).

Although we have not used the subscript λ with the reflectance quantities discussed here, they are functions of wavelength. They can be integrated over the passband of a satellite radiometer or over the solar spectrum. To so integrate albedo, integration is performed separately for E and M over the passband, and

TABLE 3.3. Albedo (%) of Various Surfaces Integrated over Solar Wavelengths[a]

Bare soil	10–25
Sand, desert	25–40
Grass	15–25
Forest	10–20
Snow (clean, dry)	75–95
Snow (wet and/or dirty)	25–75
Sea surface (sun > 25° above horizon)	<10
Sea surface (low sun angle)	10–70

[a] Adapted from Kondratyev (1969) by Wallace and Hobbs (1977).

then the ratio is taken. Readers of the literature should be careful to determine whether "albedo," in particular, refers to a monochromatic quantity or to one integrated over some passband. The albedo of various surfaces, integrated over solar wavelengths, is given in Table 3.3.

A function closely related to albedo and bidirectional reflectance is the *anisotropic reflectance factor*

$$\xi_r(\theta_r,\phi_r;\theta_i,\phi_i) \equiv \frac{\pi}{A}\gamma_r(\theta_r,\phi_r;\theta_i,\phi_i). \tag{3.67}$$

Suppose a non-Lambertian surface has albedo A. ξ_r compares the radiance from the surface to that from a Lambertian surface also with albedo A; it is greater than one where the surface reflects more than a Lambertian surface; it is less than one where the surface reflects less than a Lambertian surface. Since bidirectional reflectance is usually applied to solar radiation, it is convenient to use the azimuth angle of the sun as the reference azimuth. ξ_r is therefore usually written as $\xi_r(\theta_r, \theta_{sun}, \phi_r - \phi_{sun})$. Figure 3.22 shows ξ_r for four surfaces: snow, cloud, land, and ocean. Note that although isotropic reflection ($\xi_r \approx 1$) is not a bad assumption in some cases, sun glint is evident in the water reflectance. Most surfaces deviate significantly from Lambertian surfaces at low solar elevation angles (high solar zenith angles). Finally, note that Eqs. 3.66 and 3.67 require that for any incident direction $(\theta_{sun},\phi_{sun})$

$$\int_0^{2\pi}\int_0^{\pi/2} \xi_r(\theta_r, \phi_r; \theta_{sun}, \phi_{sun}) \cos\theta_r \sin\theta_r \, d\theta_r \, d\phi_r \equiv \pi. \tag{3.68}$$

This equation is useful for checking experimentally determined values of ξ_r.

3.7 SOLAR RADIATION

The solar radiation reaching the Earth originates (for our purposes) from a layer of the sun called the *photosphere*, which coincides with the visible disk of

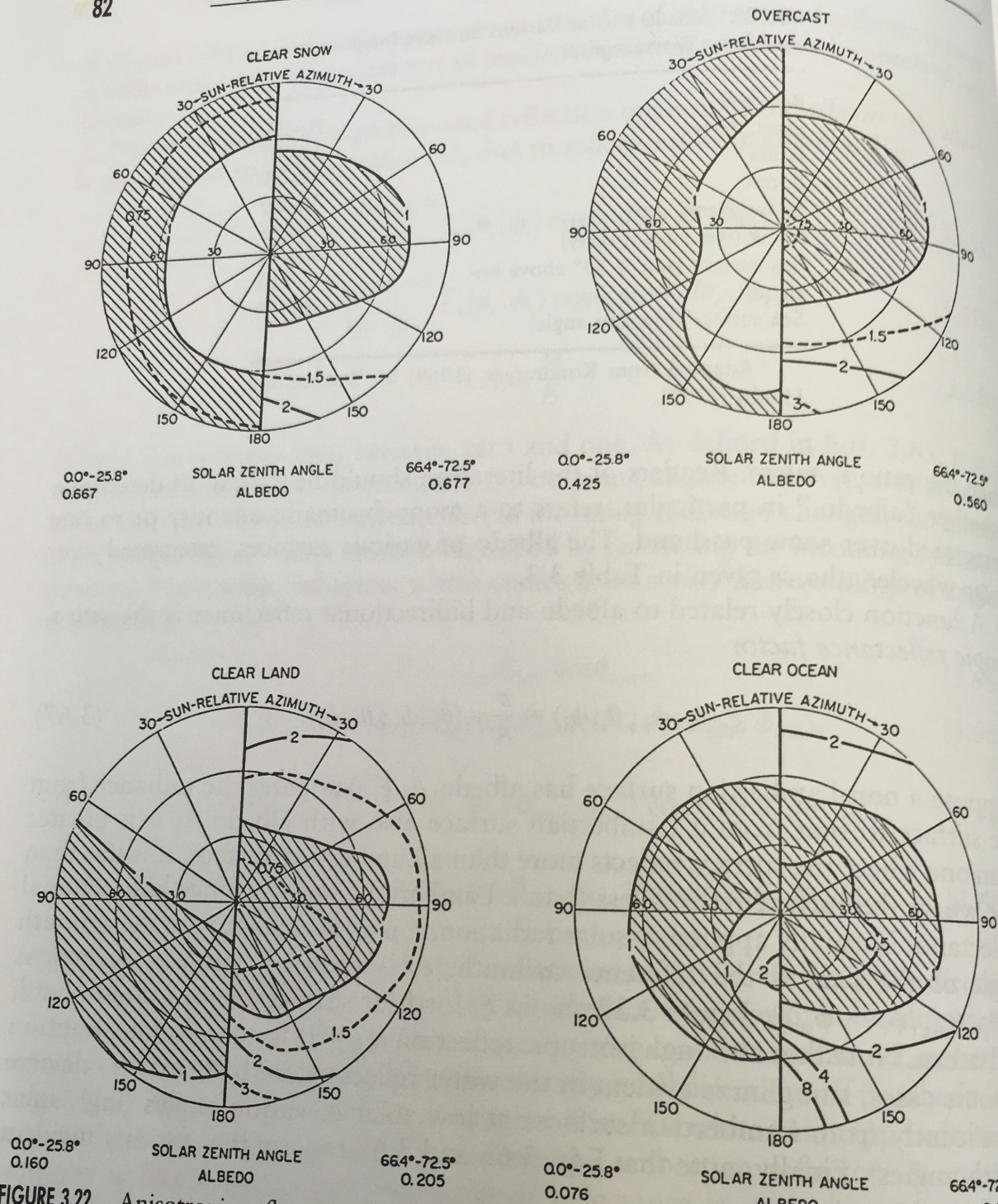

FIGURE 3.22. Anisotropic reflectance factor for snow, middle cloud (overcast), clear land, and clear ocean from the Nimbus 7 Earth Radiation Budget Experiment. The radial lines represent the viewing azimuth angle relative to the sun: At the top of each plot (0° relative azimuth), reflection is back toward the sun; at the bottom of each plot (180° relative azimuth), reflection is away from the sun. The circles represent the viewing zenith angle: The center (0° zenith angle) is looking straight down on the scene; the outer circle (90° zenith angle) represents viewing parallel to the surface. Shaded areas are those in which the scene reflects less radiation (appears darker) than an isotropic (Lambertian) reflector; unshaded areas reflect more radiation (appear brighter) than an isotropic reflector. [Plotted from data in Suttles *et al.* (1988).]

the sun and has a radius of 6.96×10^5 km. The radiation leaving the photosphere is very nearly that of a 6000-K blackbody. However, before reaching Earth, solar radiation must traverse the solar atmospheric layers of the *chromosphere* and the *corona*. The gases in these layers are both cooler and warmer than 6000 K; therefore, they both absorb and emit radiation at their characteristic wavelengths. After leaving the solar atmosphere, the radiation travels (on average) the 1.49598×10^8 km to Earth. Because the solid angle subtended by the sun at the Earth is so small (6.8×10^{-5} sr) solar radiation all comes from essentially the same direction. It is customary, therefore, to use solar irradiance rather than solar radiance. The irradiance reaching the top of the Earth's atmosphere is the radiant exitance leaving the top of the sun's atmosphere times the square of the ratio of the radius of the photosphere to the Earth–sun distance ($L_{sun}\Omega_{sun}$). The radiation reaching the Earth's surface is further modified by scattering and gaseous absorption in the atmosphere. Figure 3.23 shows the solar spectral irradiance reaching the top of the Earth's atmosphere and that reaching the surface. Shown for comparison is the spectral irradiance which would reach the Earth if the sun were a 6000-K blackbody.

Solar irradiance reaching the Earth peaks in the visible portion of the spectrum near 0.48 μm, whereas infrared radiation emitted by the Earth peaks near 10 μm. The Earth emits essentially no visible radiation; likewise, the Earth receives negligible amounts of 10 μm solar radiation, due to a combination of the sun's

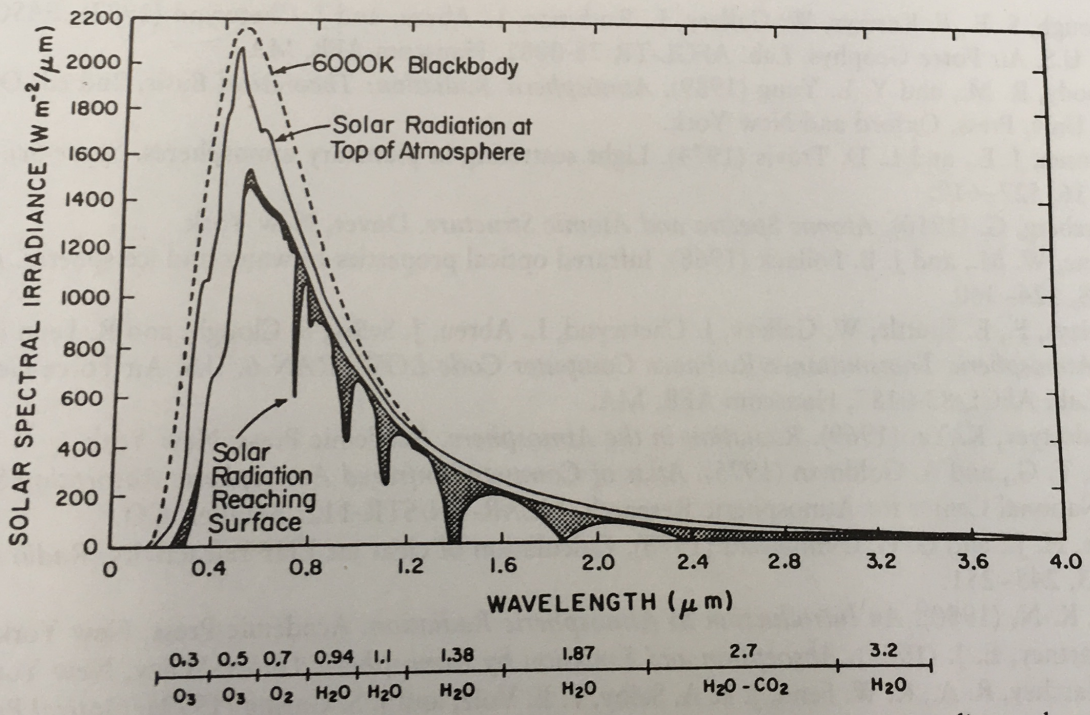

FIGURE 3.23. Solar spectral irradiance. The dashed curve shows the approximate irradiance that would be received at the Earth if the sun were a 6000-K blackbody. The top solid curve shows the spectral irradiance at the top of the atmosphere. (The integral under this curve is the solar constant.) The bottom solid curve represents the approximate solar irradiance reaching the Earth's surface after absorption and scattering in the atmosphere. The shaded area represents absorption by atmospheric gases, and the difference between the top solid curve and the envelope of the shaded area represents scattering. [Adapted from Liou (1980). Reprinted by permission of Academic Press.]

temperature and its very great distance from Earth. As a result of this separation in wavelength, solar radiation is often called *shortwave radiation*, and terrestrial radiation is called *longwave radiation*. The separation between solar and terrestrial radiation is not quite complete, however. Suppose that we represent the Earth as a 250-K blackbody and that we represent the sun as a black, 5774-K sphere whose radius is that of the sun and whose distance is the mean Earth–sun distance. Then solar radiation and terrestrial radiation are equal in magnitude at about 5.7 μm. Solar radiation is one tenth terrestrial radiation at 7.7 μm, and terrestrial radiation is one tenth solar radiation at 4.5 μm. During daylight hours, satellite data must be carefully interpreted near these wavelengths.

The annual average total irradiance reaching the top of the Earth's atmosphere is known as the *solar constant* (S_{sun}). Accurate determination of the solar constant is important for solar physics and astronomy as well as meteorology. Several satellites are currently making measurements of the solar constant. A "consensus" value of S_{sun}, based on satellite radiometer measurements,[20] is about 1368 W m^{-2} (equivalent to a 5774-K blackbody). Unfortunately the solar "constant" is not constant. It appears to follow the 11-year sunspot cycle, varying about $\pm$0.6 W m^{-2} (see Section 10.1). Of course the solar irradiance varies $\pm$3.4% from S_{sun} during the year due to the eccentricity of the Earth's orbit about the sun.

Bibliography

Clough, S. F., F. Kneizys, W. Gallery, L. Rothman, L. Abreu, and J. Chetwynd (1982). *FASCOD.* U.S. Air Force Geophys. Lab. AFGL-TR-78-0081, Hanscom AFB, MA.

Goody, R. M., and Y. L. Yung (1989). *Atmospheric Radiation: Theoretical Basis*, 2nd ed. Oxford Univ. Press, Oxford and New York.

Hansen, J. E., and L. D. Travis (1974). Light scattering in planetary atmospheres. *Space Sci. Rev.*, 16, 527–610.

Herzberg, G. (1950). *Atomic Spectra and Atomic Structure*. Dover, New York.

Irvine, W. M., and J. B. Pollack (1968). Infrared optical properties of water and ice spheres. *Icarus*, 8, 324–360.

Kneizys, F., E. Shuttle, W. Gallery, J. Chetwynd, L. Abreu, J. Selby, S. Clough, and R. Fenn (1983). *Atmospheric Transmittance/Radiance Computer Code LOWTRAN 6*. U.S. Air Force Geophys. Lab. AFGL-83-0187, Hanscom AFB, MA.

Kondratyev, K. Ya. (1969). *Radiation in the Atmosphere*. Academic Press, New York.

Kyle, T. G., and A. Goldman (1975). *Atlas of Computed Infrared Atmospheric Absorption Spectra.* National Center for Atmospheric Research, NCAR-TN/STR-112, Boulder, CO.

Liebe, H. J., and G. G. Gimmestad (1978). Calculation of clear air EHF refractivity. *Radio Science*, 13, 245–251.

Liou, K.-N. (1980). *An Introduction to Atmospheric Radiation*. Academic Press, New York.

McCartney, E. J. (1983). *Absorption and Emission by Atmospheric Gases*. Wiley, New York.

McClatchey, R. A., R. W. Fenn, J. E. A. Selby, F. E. Volz, and J. S. Garing (1972). *Optical Properties*

[20] Based on measurements from the Nimbus 7 Earth Radiation Budget (ERB) experiment, the Active Cavity Radiometer Irradiance Monitor (ACRIM) on board the Solar Maximum Mission satellite, and the Earth Radiation Budget Experiment (ERBE) on board the Earth Radiation Budget Satellite, NOAA 9, and NOAA 10. A systematic difference between the instruments of approximately 7 W m^{-2} has yet to be resolved (see Section 10.1).

of the Atmosphere (3rd ed.). U.S. Air Force Cambridge Res. Lab. AFCRL-TR-72-0497, Hanscom AFB, MA.

McClatchey, R. A., W. S. Benedict, S. A. Clough, D. E. Burch, R. F. Calfee, K. Fox, L. S. Rothman, and J. S. Garing, (1973). *AFCRL Atmospheric Absorption Line Parameters Compilation*. U.S. Air Force Cambridge Res. Lab. AFCRL-TR-73-0096, Hanscom AFB, MA.

McMillin, L. M., and H. E. Fleming (1976). Atmospheric transmittance of an absorbing gas: A computationally fast and accurate transmittance model for absorbing gases with constant mixing ratios in inhomogeneous atmospheres. *Appl. Optics*, 15, 358–363.

Raschke, E. (ed.), (1978): *Terminology and Units of Radiation Quantities and Measurements*. International Association of Meteorology and Atmospheric Sciences (IAMAS, formerly the International Association of Meteorology and Atmospheric Physics) Radiation Commission, Boulder, CO. (Printed by the National Center for Atmospheric Research, Boulder, CO 80307.)

Smith, W. L. (1985). Satellites. In D. D. Houghton (ed.), *Handbook of Applied Meteorology*. John Wiley & Sons, Inc., New York.

Suttles, J. T., R. N. Green, P. Minnis, G. L. Smith, W. F. Staylor, B. A. Wielicki, I. J. Walker, D. F. Young, V. R. Taylor, and L. L. Stowe (1988). *Angular Radiation Models for Earth-Atmosphere System, Volume I: Shortwave Radiation*. NASA Ref. Pub. RP 1184, vol. I, Langley Research Center, Hampton, VA.

Valley, S. L. (ed.) (1965). *Handbook of Geophysics and Space Environments*. Air Force Cambridge Research Laboratory, Hanscom AFB, MA.

van de Hulst, H. C. (1957). *Light Scattering by Small Particles*. John Wiley & Sons, New York.

Wallace, J. M., and P. V. Hobbs (1977). *Atmospheric Science: An Introductory Survey*. Academic Press, New York.

Welch, R. M., S. K. Cox, and J. M. Davis (1980). Solar radiation and clouds. *Meteorol. Monogr.*, 17, 96 pp.